ORIENTATIONAL AND FREQUENCY EFFECTS ON WHOLE ANIMAL ABSORPTION OF RF ENERGY*

O. P. GANDHI

(*Electrical Engineering Department, University of Utah, Salt Lake City, Utah*)

Received on April 10, 1974

ABSTRACT

A parallel plate waveguide (WG) is used to determine wideband (285–4000 MHz) absorption characteristics of prolate spheroidal bodies of aspect ratios (a/b) up to and including 5·75 (the value taken for humans). The measurements are done for $\hat{E} \parallel \hat{a}$, $\hat{H} \parallel \hat{a}$, and $\hat{k} \parallel \hat{a}$ orientations, these corresponding to the major length (2 a) of the body, respectively, along the electric and magnetic fields and the propagation vector. The validity of the method is checked by comparing the WG measurements with those of free space irradiation and also from the correlation with Mie theory of the absorption characteristics of biological-phantom spheres. For 96, 158, 261, 390 gm rats in $\hat{k} \parallel \hat{a}$ orientation, maximum is observed at frequencies of 1217, 1020, 900 and 760 MHz, respectively. The frequencies of peak absorption and the values thereat demonstrate $W^{-1/3}$ and $W^{2/3}$ dependences, respectively, upon weight W of the animal. Experiments with animals and prolate spheroids demonstrate a considerably larger absorption in the $\hat{E} \parallel \hat{a}$ than in the $\hat{H} \parallel \hat{a}$ orientation, with $\hat{k} \parallel \hat{a}$ orientation giving a value only slightly larger than that for $\hat{H} \parallel \hat{a}$ configuration. Peak absorption in the $\hat{E} \parallel \hat{a}$ configuration occurs at a frequency such that $ka \simeq 0·75$ to $1·0$. Maximum absorption for $\hat{k} \parallel \hat{a}$ and $\hat{H} \parallel \hat{a}$ orientations occurs at successively higher frequencies with ka for these frequencies on the order of a/2b. RF absorption larger by an order of magnitude or more is found to occur at resonance for $\hat{E} \parallel \hat{a}$ than for other orientations.

O. P. GANDHI

1. INTRODUCTION

This paper addresses the following questions:

1. What, if any, is the frequency dependence of RF absorption of biological systems such as whole animals? Are there frequency ranges where a larger percentage of plane wave incident power is absorbed in the body, resulting thereby in an increased hazard for a given incident power density?

2. What, if any, are the effects of the various orientations of the animal on total power absorption in plane wave fields? Since most biological systems have different overall dimensions along the three orthogonal axes docs the orientation of the incident electric field relative, say, to the longest dimension of the animal affect the total power absorption in the body?

3. Can one extrapolate to predict frequency regions of most interest from the point of view of maximum absorption in different orientations for the whole man or important subparts thereof?

Prior knowledge on the above subjects consists of theoretical studies on homogeneous lossy spheres [1–3] of dielectric properties matching biological tissues with high water content such as muscle and brain matter. Using Mie theory [4] maximum absorption is predicted [1] for a frequency f such that $ka = 2\pi fa/c$ is on the order of $0\cdot5$ where a is radius of the sphere and c the velocity of light in free space. Recognizing that most biological systems have different dimensions along the three axes, a theory [5] has recently been developed for homogeneous lossy prolate spheroids of different aspect ratios to more closely match the overall dimensions of various animals. The analysis which is considerably more realistic than the spherical model approximation is valid in the low frequency ($ka \leqslant 0\cdot3$) approximation and does not consequently predict regions of resonance or maximum absorption in bodies of prolate spheroidal shape. Also, to our knowledge, no experimental data exist todate to confirm the validity of this theory.

An important motivation in undertaking the study reported in this paper was a recent study [6] conducted at Walter Reed Institute of Research on the frequency effects of microwave irradiation in behavioural performance of Wistar rats. Using the time elapsed from the onset of radiation to work stoppage as the criterion, animals, both male and female, were exposed to plane wave fields of power densities of 50, 75, 100 and 150 mW/cm² at frequencies of 750, 1700, 2450 and 3000 MHz. The animals, contained in ¼" clear plexiglass containers of dimensions 12" long, 12" high, and 10"

wide, received a pellet of food for every ten presses on a response bar. The animals' exposure to microwaves was such that the waves were incident, mostly broadside to the animals. For each of the incident power densities, microwaves at 1700 MHz were found to be more effective than radiation at 2450 MHz, which in turn was more effective than exposure at 3000 MHz in reducing time to work stoppage. The exposure at 1700 MHz was also found to result in a lower time to work stoppage than that at 750 MHz. This frequency behavior of power at 1700 MHz, being more effective than that at the other three frequenies, was found for both males and females of the species.

In order to understand this rather unexpected result, and recognizing the sparseness of the frequencies used, it was decided to develop a procedure for determining the RF absorption spectrum of whole animals or parts thereof to plane wave fields. Noting that TEM waves in parallel plate lines have field configuration similar to that of plane waves and that such guides, unlike rectangular and cylindrical waveguides, are broadband and capable of working down to low RF frequencies, this was the approach taken toward the aforementioned problem. This paper describes the design details of the measuring system and the experimental results of whole animal absorption characteristics of 96, 158, 261, 390 gram rats over a frequency region from 285 to 4000 MHz. The validity of using a parallel plane line to determine plane wave absorption characteristics is confirmed by measuring the absorption characteristics of lossy spheres and the excellent correlation of the results so observed with those from Mie theory [1]. The system was used, too, to determine the absorption characteristics, including the all important peak absorption or resonance regions, for prolate spheroids of several aspect ratios a/b (ratio of dimensions along major and minor axes) from 2 to 5·75 (the value 5·75 taken to be that for humans). An important result of the study on prolate spheroids was to point out that overall absorption in $\hat{E} \parallel \hat{a}$ configuration of such bodies is considerably higher than that in $\hat{H} \parallel \hat{a}$ configuration, with $\hat{K} \parallel \hat{a}$ orientation resulting in values only a little higher than those for $\hat{H} \parallel \hat{a}$ orientation. This is in qualitative agreement with the results of the small ka theory of Ref. 5. Furthermore, from our experiments, it was found that invariably the peak absorption frequency of the $\hat{E} \parallel \hat{a}$ configuration is the lowest of the three orientations, with $\hat{k} \parallel \hat{a}$ and $\hat{H} \parallel \hat{a}$ orientations taking successively higher resonance frequencies. The absorption curves for bodies of prolate spheroidal

shapes for the three orientations are qualitatively sketched in Fig. 1. As seen therein, in the frequency region corresponding to that for peak absorption in the $\hat{E} \parallel \hat{a}$ configuration, the RF absorption in that orientation may be as much as an order of magnitude or more larger than that for the other orientations. Using the parallel plate system, variation similar to that of Fig. 1 has been measured, too, for a 25 gm mouse, confirming thereby the advantage of using prolate spheroidal shapes to understand the frequency and orientational effects on RF absorption in biological systems.
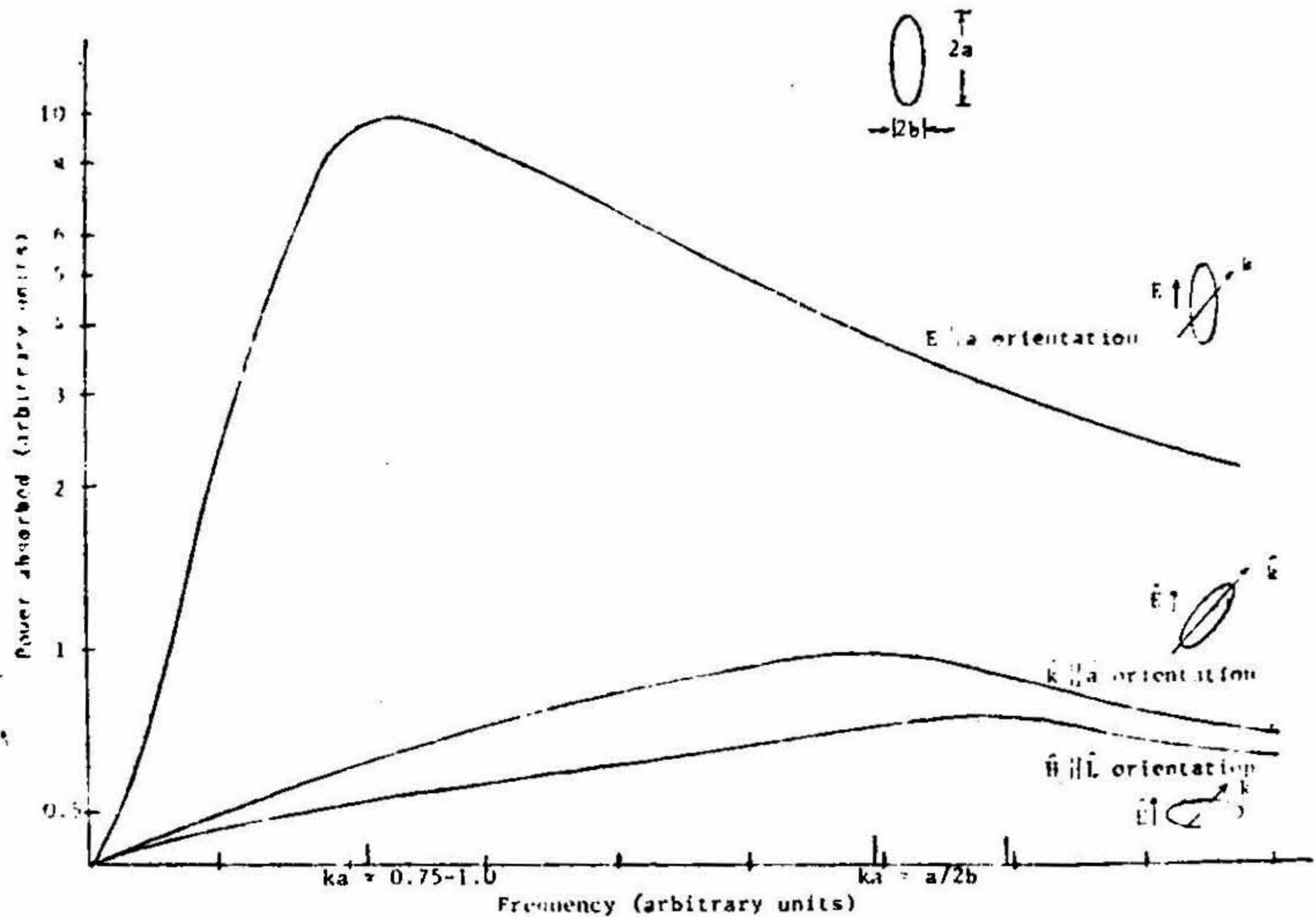
FIG. 1. Typical RF absorption curves for animals and bodies of prolate spheroidal shape.

The main features of the foregoing have been confirmed by the alternative experiments of heating prolate spheroids by plane waves radiated from a horn in an anechoic chamber and examining the temperature enhancement by thermometry and by thermography. An excellent correlation between the results of the WG measurements and those of free space irradiation is observed which testifies to the viability of using a parallel plate waveguide as a simple method of determining absorption characteristics. While further experiments need to be done with different biological bodies at the appropriate $\hat{E} \parallel \hat{a}$ resonance frequencies, initial testing of 25 gm mice at 1700 MHz (at a frequency considerably off their $\hat{E} \parallel \hat{a}$ resonance frequency)

showed a time to lethality of about 60 per cent in the $\hat{E}^+\hat{a}$ orientation as compared to that in the $\hat{H} \parallel \hat{a}$ configuration.

2. THE PARALLEL PLATE LINE

In order to determine the plane wave RF absorption characteristics of biological bodies, it is necessary to work with waveguides rather than horns radiating into free space simulated by anechoic chambers both because of the lower power requirement and the ease of obtaining the total power absorbed in the system. For studies over widebands, it is also essential that such waveguides be capable of propagation down to megacycle frequencies and carrying power in the TEM mode similar in fields configuration to those of plane waves. The waveguides that fit this requirement are the coaxial line, the triplate line, and the parallel plate line. In order to maintain the symmetry of the line, it is necessary to use two identical bodies placed above and below the center conductor in both the coaxial and the triplate lines. It was consequently decided to use a parallel plate line. There was some concern, however, of the radiation losses from such a line because of the open sides and the possibility of exciting higher order modes, particularly at higher frequencies. This concern has been diminished to some extent by the correlation of the WG results with those of free space irradiation and by an excellent agreement of the measured characteristics of biological-phantom spheres with the results of the Mie theory [1].

In order to conduct measurements with Wister rats as the test animals the parallel plate waveguide is designed with a cross section of $6\cdot35 \times 15\cdot9$ cm². This is to assure that even the largest 390 gm rats do not overly fill the waveguide in their $\hat{K} \parallel \hat{a}$ orientation. It was found in actual practice that waveguide dimensions should be such that the bodies to be measured fill between 10–30 per cent of the cross section for best results. For such cases the insertion loss is on the order of 1 *dB* or more so that the measurement errors of the microwave network analyzer are minimized by comparison. Since the Amphenol UG-58/U coaxial connectors are 50-ohm and the line of the above dimensions has a characteristic impedance [7] of 80 ohms, gradual taper over a length of 30 centimeters at each end is used for impedance matching. A uniform central section of 30 centimeters is used to allow placement of bodies for insertion loss measurements. The sketch of the line and its photograph are shown in Fig. 2. The ground plane or the lower plate has a width of $20\cdot3$ cm, a somewhat larger value than the upper plate to allow for the region of fringing fields. Using the HP8410Å

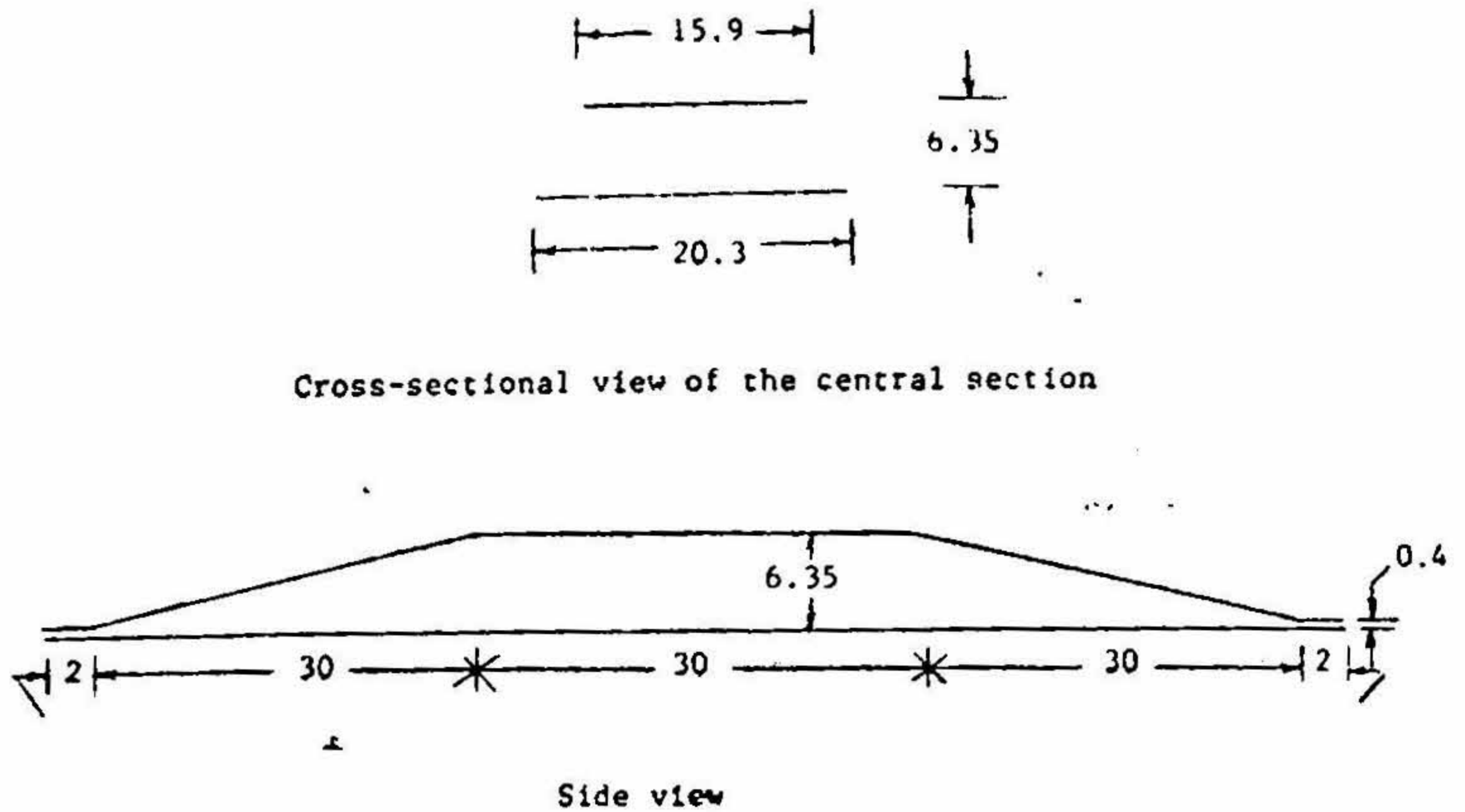Cross-sectional view of the central section

Side view

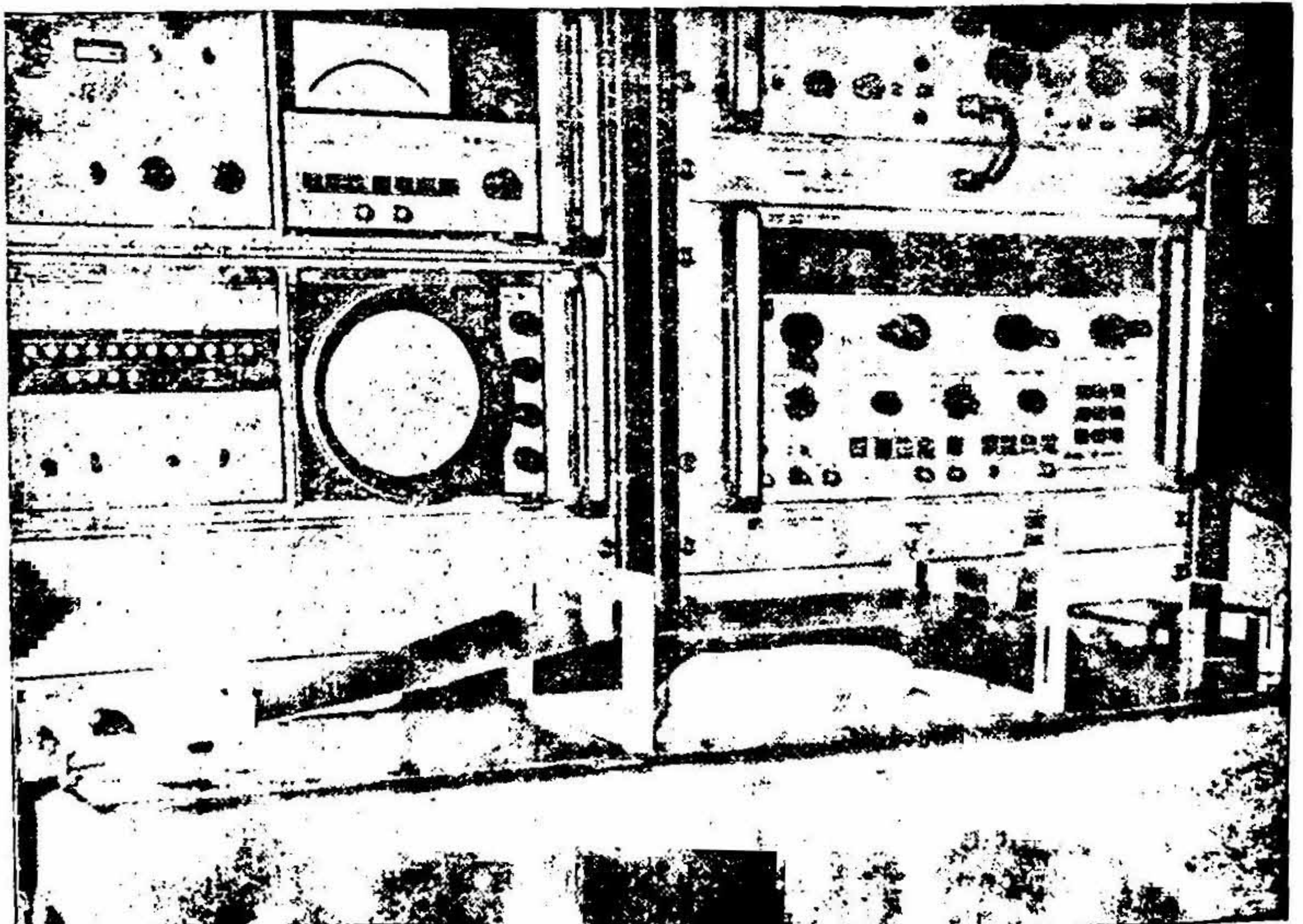FIG. 2 (a). Sketch of the parallel plate wave guide (dimensions in cm).

FIG. 2 (b). Photograph of the parallel plate waveguide used for measuring plane wave absorption characteristics of biological systems.

network analyzer to span the 285 to 4000 MHz band in 100 frequency steps, a set of 15 measurements is taken and a statistical analysis performed thereupon using an on-line HP2116B computer. The values for the VSWR, mean insertion loss, standard deviation, the least and the largest values of attenuation as measured at different frequencies are then printed out. Additional attenuation (insertion loss) in the line due to the inserted body together with the standard deviation is plotted over the 285–4000 MHz band or any part thereof as desired.

The first measurement performed was to determine the power transmission characteristics of the empty waveguide, hereinafter called the WG. Using frequency steps of 35 MHz, the insertion loss and VSWR of the WG are measured and are plotted in Fig. 3 for the frequency band 285 to 2000 MHz. As seen from the figure, the VSWR is less than 1·45 over the entire band. The attenuation as high as 5·0 dB at higher frequencies is considerably more than 0·0 dB [8] that may be calculated for copper losses. The additional attenuation may be ascribed to possible radiation from the open ends of the WG particularly at higher frequencies. Using input powers on the order of 500 mW, a field intensity of no more than 0·5 mW/cm^2 could be measured at a distance of 5 centimeters from the open ends of the WG.
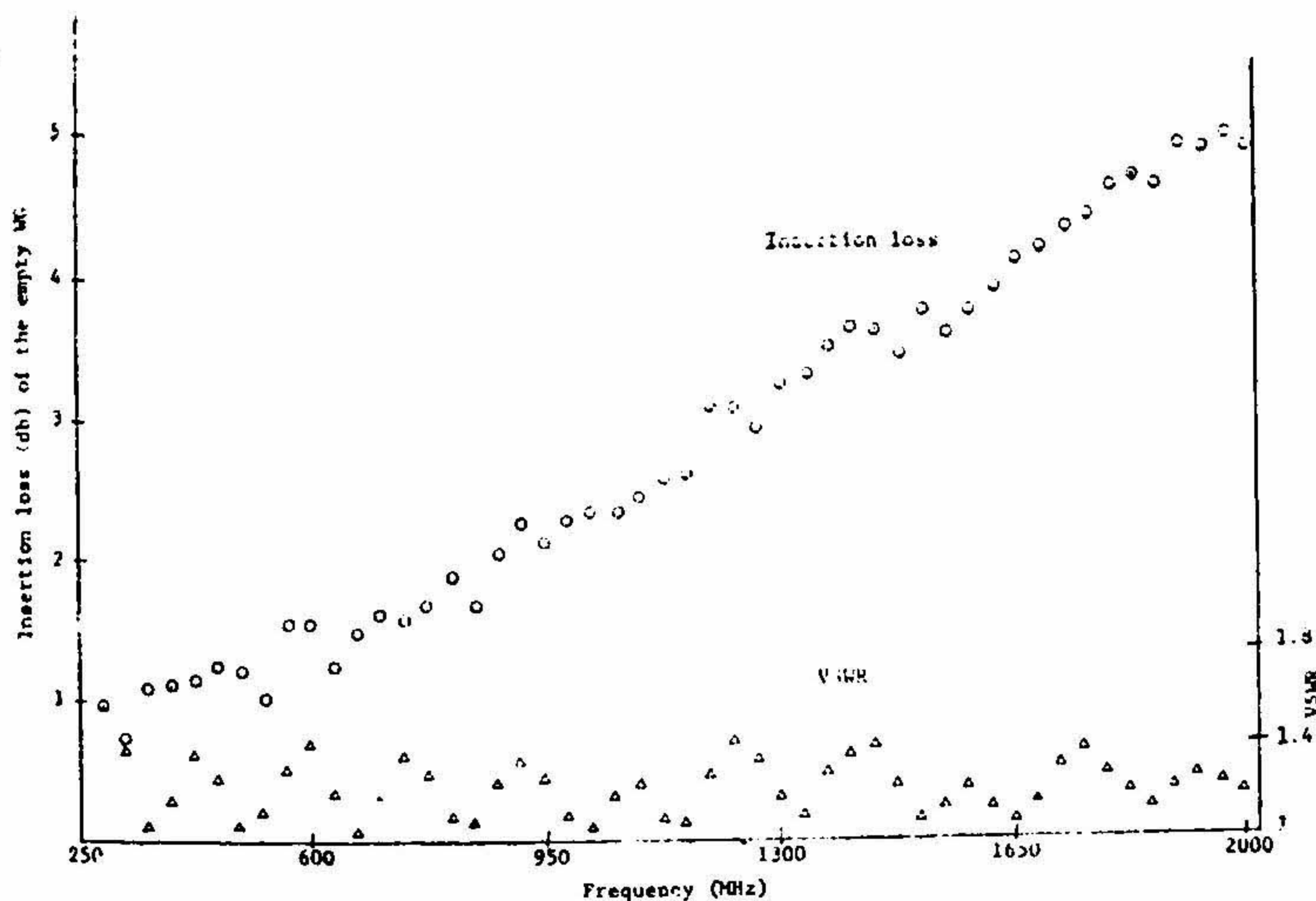

FIG. 3. Insertion loss and VSWR of the "uncorrected" empty WG.

For most of the measurements (with the network analyser), power levels on the order of 1 mW have, however, been used and field intensities out of the WG are proportionately lower.

It may be mentioned here that while the parallel plate WG is extremely broadband and consequently convenient to use for determining the first-shot absorption characteristics of various bodies and, as will be seen later, gives a fairly accurate picture of the regions of peak absorption, a more accurate determination in the resonance regions so located may well be done by completely enclosed (and consequently non-radiating) TEM waveguides. One such waveguide [9] is the dielectric loaded rectangular waveguide capable of exciting TEM waves at essentially a single frequency dependent upon the dimensions of the line and the dielectric fillers. It is felt that quasi-TEM propagation may be assumed in such waveguides over narrow bands designed to coincide with the resonance regions of most interest determined in the first instance by the parallel plate WG. This should help to avoid the handicap of possible radiation from the WG and thus allow more accurate measurements of the insertion loss in the resonance region. Rectangular versions of coaxial lines [10] presently used at megacycle frequencies may also be usable at high frequencies, but the loading would be trickier if one is to avoid the excitation of higher order modes. The dimensions of such lines ($2 \times 9\,m^2$ for the center conductor alone) as presently used are also unwieldy, and small single animals placed in such a waveguide would produce an additonal attenuation too small for accurate measurements.

Using the empty WG for the "connect through" in the calibration of the network analyzer HP8410A, the base attenuation and reflection may be accounted for in subsequent measurements. Using this method the insertion loss of the empty WG, as so cancelled, is measured to be within $\pm 0\cdot 1dB$ with VSWR less than $1\cdot 042$ over the 285–2000 MHz band of the HP8745A S-parameter test set. For the HP8743A test set used in the 2000–4000 MHz band, the corresponding values are within $\pm 0\cdot 05\ dB$ for the corrected insertion loss with VSWR less than $1\cdot 017$ over the entire band. The WG so corrected for the base readings is then used for determination of (additional) insertion loss (RF absorption) due to rats, mouse, and prolate spheroids.

One of the checks performed on the measuring system was to use a $6\ dB$ coaxial pad measured previously to be $5\cdot 78$–$6\cdot 00\ dB$ (VSWR $\leq 1\cdot 057$) over the 285–2000 MHz band, using the flexible coaxial lines for the connect-through. Connecting this pad to the input part of the WG (with its inherent loss cancelled in the calibration process), the attenuation was measured to

be 5·77 to 6·08 *dB* with VSWR less than 1·055 over the 285–2000 MHz which correlates extremely well with the values given above. The same pad connected to the output part of the WG gave 5·75 to 6·00 *dB* for attenuation with a VSWR as high as 1·820 caused by the long line effect at a limited number of frequencies. The discrepancy in the VSWR is ascribed to the VSWR inherent to the WG and the inability of the computer to cancel two comparable reflections with different phases. We should hasten to add, however, that the VSWR of all the bodies (rats, mouse, prolate spheroids, spheres, etc.) reported in this paper were mostly less than 1·2 with the negligible effect that this would represent in absorption measurements.

In order to ascertain the uniformity of fields over the cross section of the waveguide, test obstacles of lossy and metal spheres were moved within the waveguide by as much as ± 10 cm in the axial direction and ± 5 cm along the width. The obstacles were moved along the height by at least ± 2 cm and to the maximum extent possible in each case dictated by the extremity of the body occupying the region about 3 mm away from the conducting plates.

For each of the obstacles the resonance frequency and peak absorption were found to vary by no more than ± 2·5 and ± 10 per cent, respectively. A slightly larger variation in the absorbed power is due to the inherent power attenuation in the WG and the resulting variation of the powers as actually incident on the obstacles.

Another check on the validity of the measuring system was made using spheres of a lossy material* with dielectric properties identical to those of the brain tissue. It was argued that if the WG is to determine the peak absorption frequencies of the biological systems of unknown characteristics, the resonance frequencies of the spheres of diameters 3·3 to 5·6 cm should correlate in the first instance with those obtained from Mie theory [1]. The results of the measurements on the spheres of the brain-phantom material are summarized in Table I.

From the data in Table I it should be noted that for spheres, the absorption peak, varying from 974 to 1610 MHz, occurs in each case for $ka = 0·55$–$0·59$, which correlates well with the values on the order of $0·50$–$0·52$ from Mie theory [1]. Plots of insertion loss as a function of frequency for

---

* The composition of the material to simulate the dielectric properties of the brain tissue as developed in the Department of Rehabilitation Medicine, University of Washington, Seattle, is 7·01 per cent Superstuff (obtained from Whamo Manufacturing Company, San Gabriel, California), 29·8 per cent polyethylene powder, 0·5823 per cent NaCl, and 62·61 per cent water,

TABLE I

Summary of the measurements on spheres of the brain-phantom material

Sphere Diameter 2 *a* in Inches	Frequency of Peak Absorption MHz	Insertion Loss for Peak Absorption Decibels	Percentage Power Absorbed at Resonance	*ka* for Peak Absorption
1·30	1610	0·31	6·9	0·5565
1·40	1466	0·43	9·4	0·5460
1·50	1388	0·65	13·9	0·5530
1·60	1361	0·61	13·1	0·5800
1·75	1235	1·10	22·4	0·5750
1·90	1160	1·61	31·0	0·5850
2·00	1079	2·72	46·5	0·5725
2·10	1058	2·72	46·5	0·5900
2·20	974	4·80	66·9	0·5680
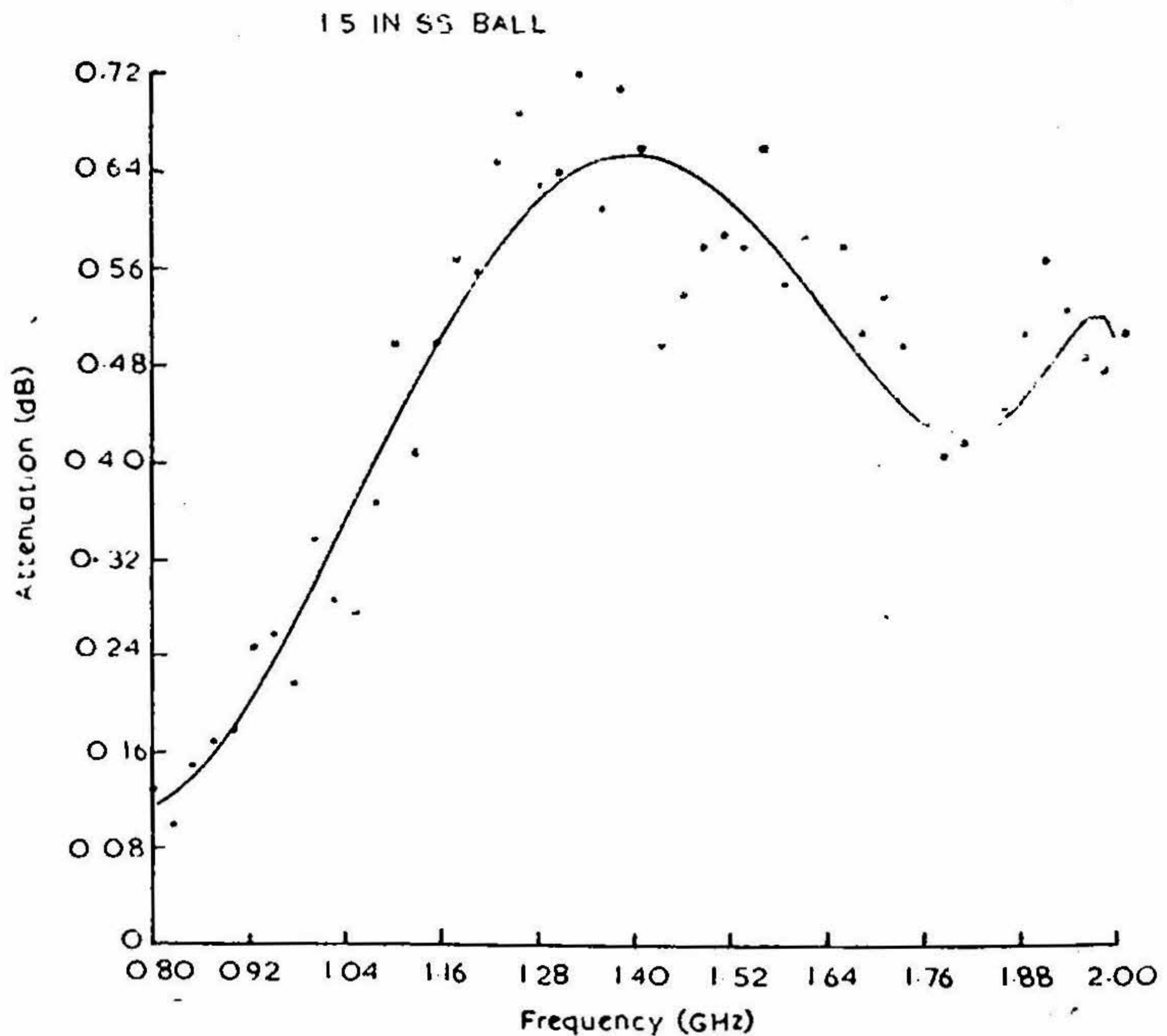
FIG. 4 (*a*). Measured insertion loss for some lossy spheres as a function of frequency.

1.75 IN. SS BALL
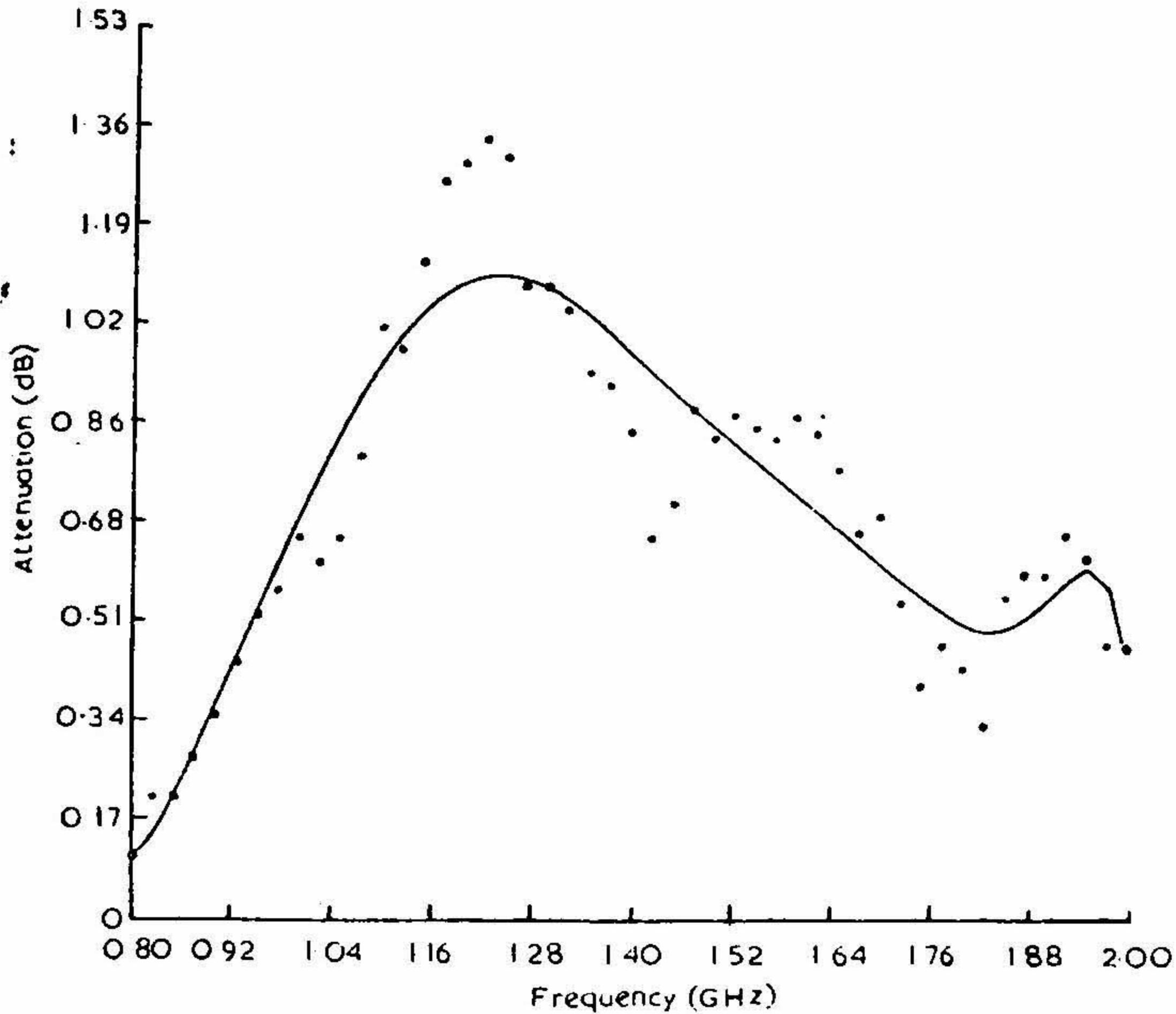
FIG. 4 (b)

some representative spheres are shown in Fig. 4. The solid curve is a 20th degree polynomial fitted to the data points by the method of least squares [11]. For low ka (below resonance) region, the power absorbed in spheres of different radii is plotted at a given frequency in Fig. 5. The absorbed power varies as $a^{6.1}$ as against a^6 from Mie theory, the result once again in excellent agreement with the theory.

The dependence of power absorbed on the frequency f is shown in Fig. 6 for spheres of different radii for the below-resonance region. The absorbed power varies as $f^{4.75}$ in reasonable correlation with f^4 dependence given from the theory. A distinction to note between the measurements and the $f^4 a^6$

O. P. GANDHI

2 IN SS BALL
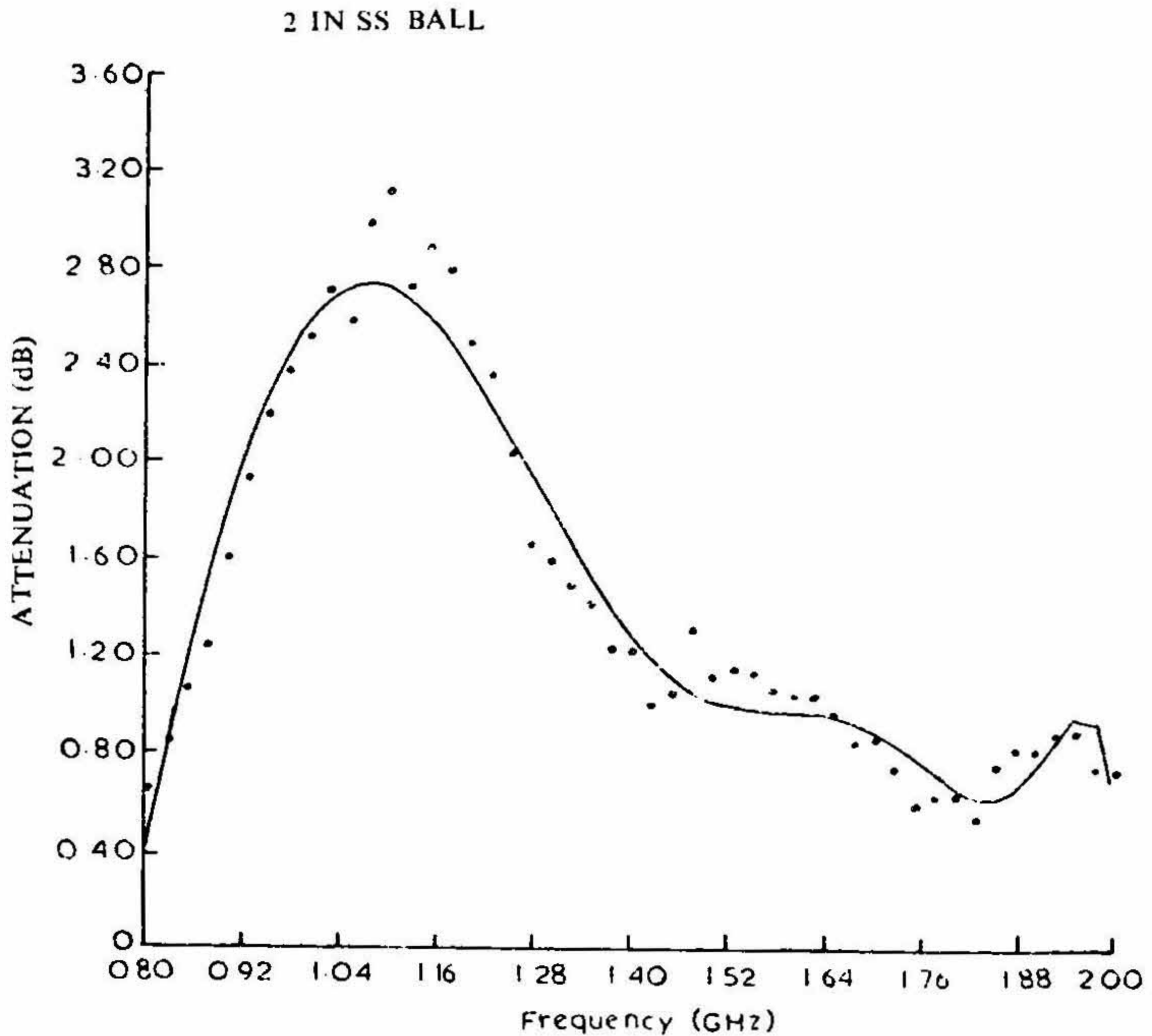
FIG. 4 (c)

dependence given from the theory is that the theory is derived for $ka \ll 1$, whereas for our measurements the value of $ka \geq 0.3$ is necessitated by the rather low insertion loss for bodies of smaller ka in the WG of the present dimensions of comparatively large width to separation ratio which results in the errors in their measurement on account of the network analyzer accuracy of ± 0.1 dB. A smaller width to separation ratio of the parallel plates would be required if low ka measurements are desired. A point of discrepancy from the theory, however, is the a^4 dependence of the peak power absorbed in the various spheres as illustrated in Fig. 5. This is puzzling in that a Sa^2 dependence is predicted in Reference 3 where S is the relative absorption coefficient.

2·2 IN DIA. SS BALL
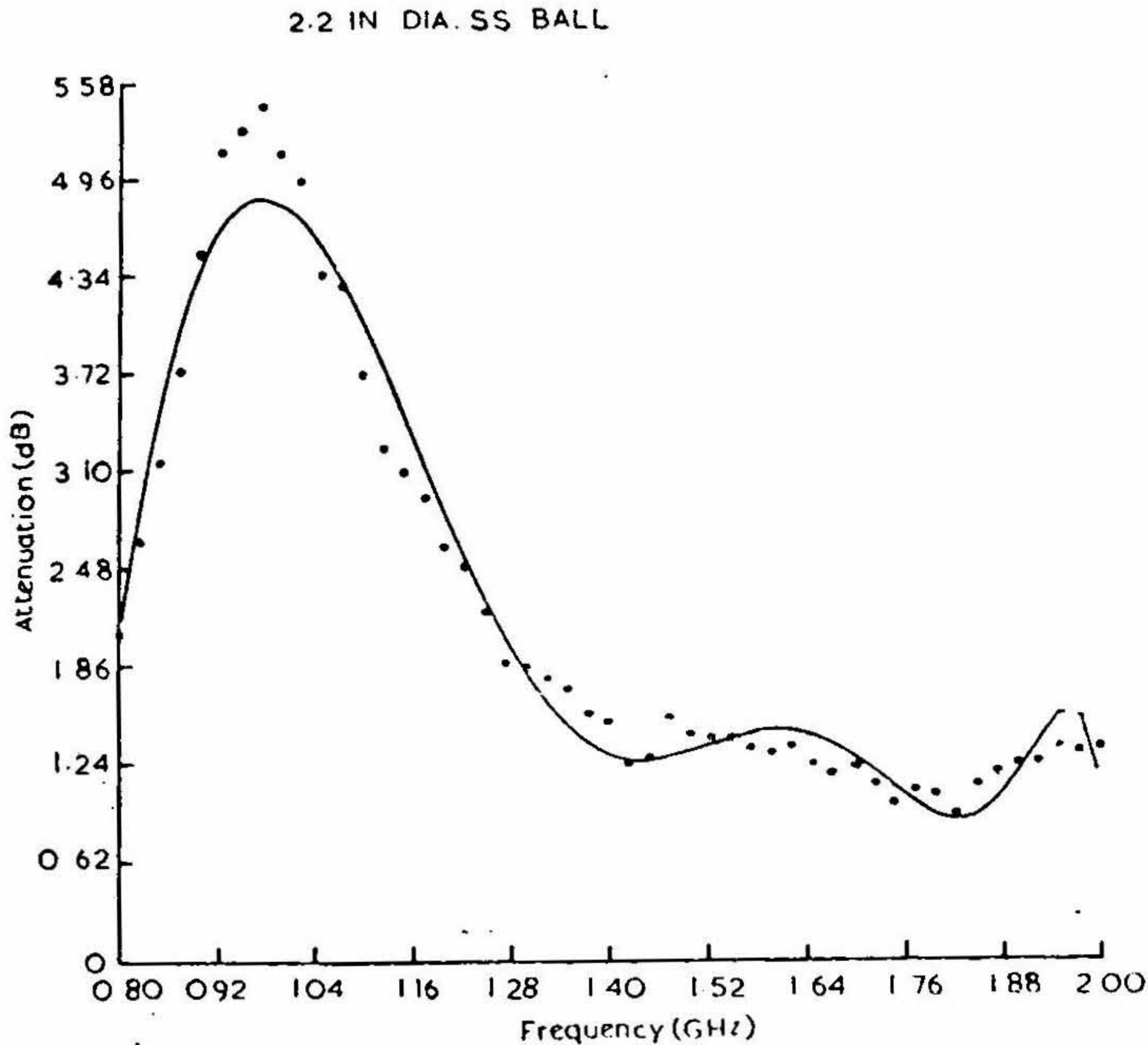
FIG. 4 (*d*)

It should be recognized, however, that the magnitude of the factor *S* has a strong dependence on the material conductivity and a strongly increasing absorption may partly be accounted for by an increasing *S* at the lower resonance frequencies characteristic of larger diameter spheres.

3. RF ABSORPTION CHARACTERISTICS OF RATS

The RF absorption of 96, 158, 261, 390 gm anesthetized rats was measured by placing the animals on a polyfoam sheet to prevent the physical contact with the plates. It was established by prior tests with test obstacles of lossy and metal spheres that the observed characteristics were fairly independent of the placement as long as the bodies were kept at a separation of 2 to 3
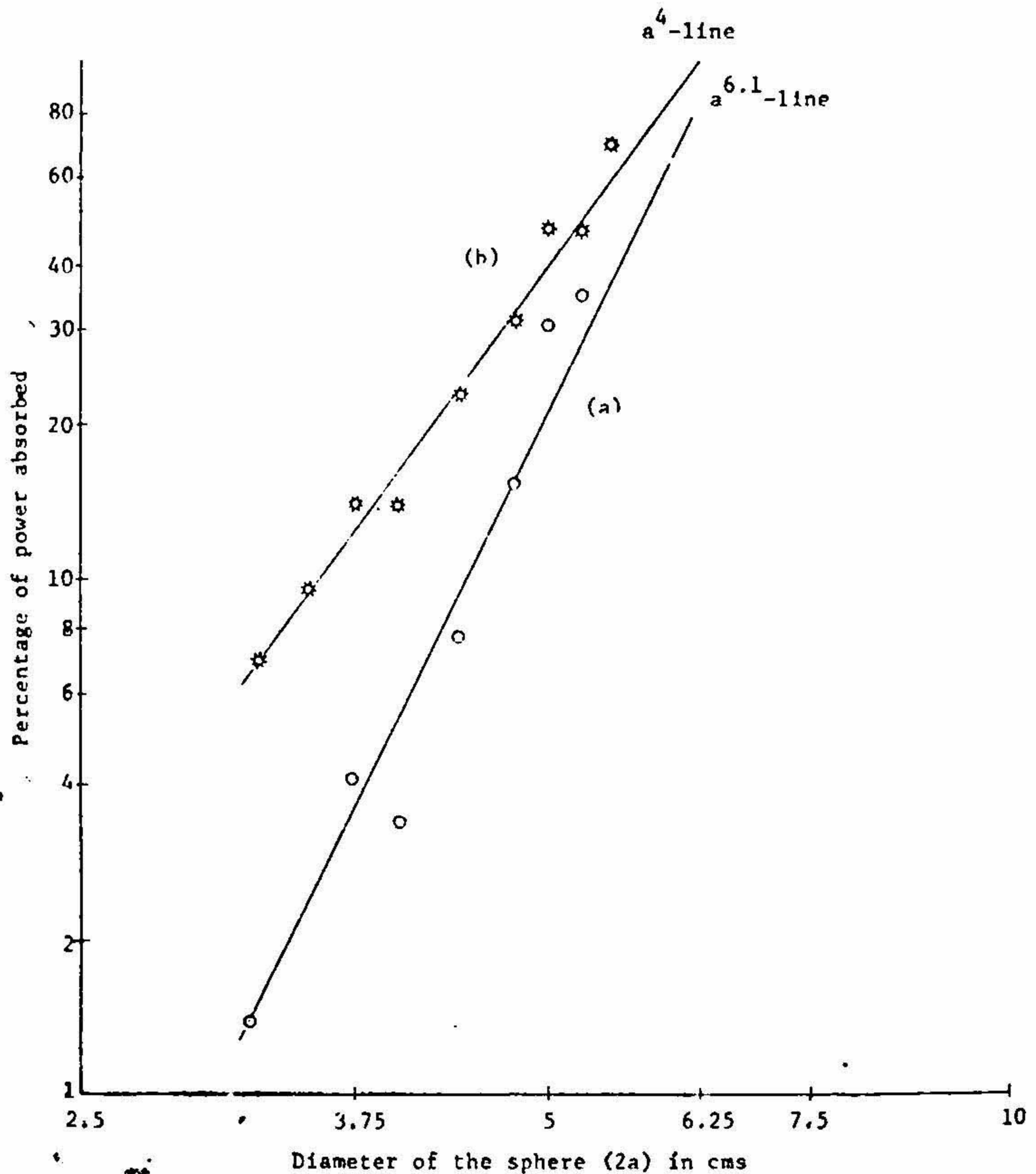
FIG. 5. RF absorption as a function of the sphere diameter. (a) Below-resonance absorption at a fixed frequency of 900 MHz. (b) At resonance absorption.

millimeters from the plates. For each of the animals, a set of 15 measurements was taken over the two frequency bands of HP8745A/HP8743A S-parameter test sets. The printout gave results of a statistical analysis performed on these measurements. The mean value of the insertion loss together with the information on standard deviation of measurements for
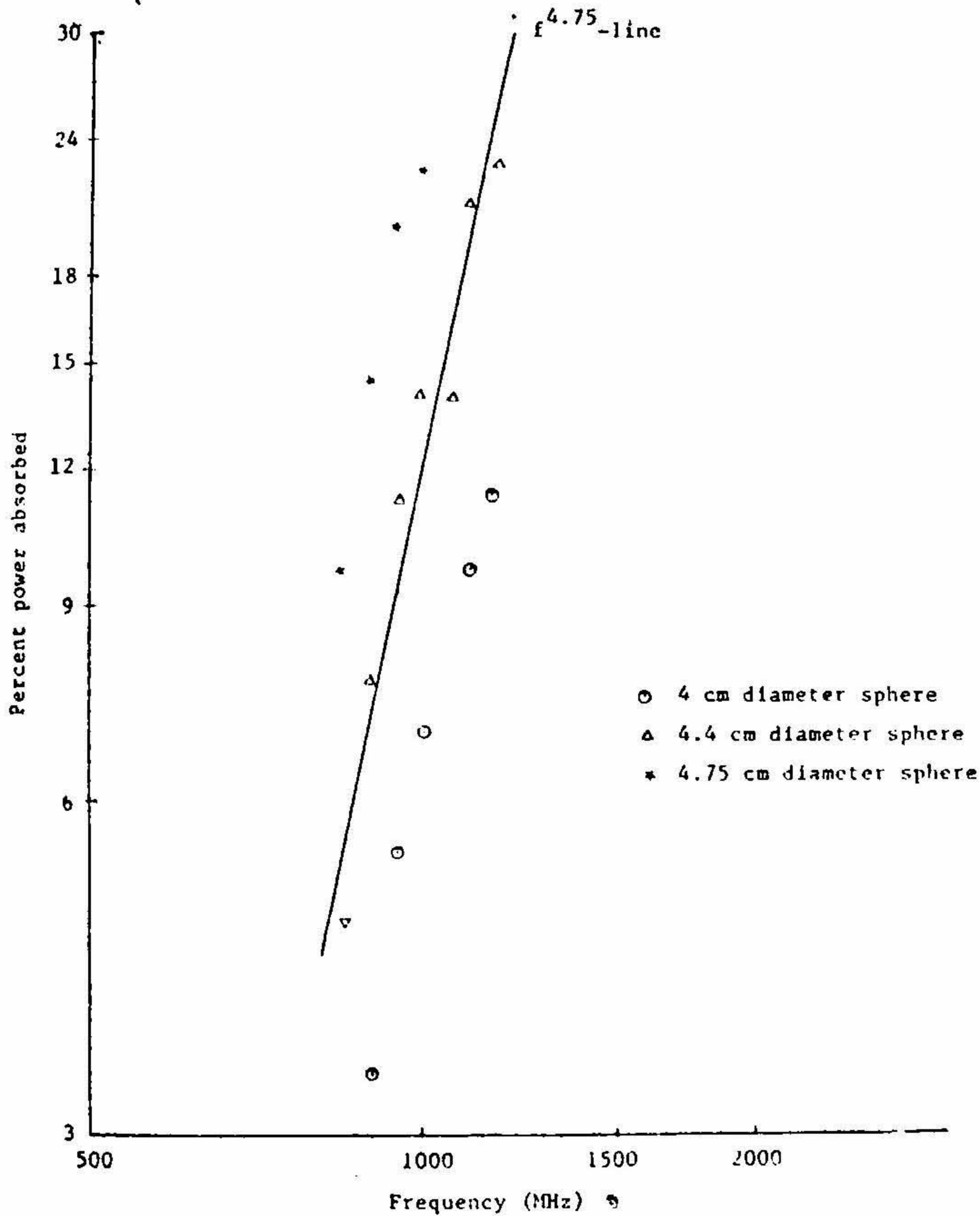
FIG. 6. Below resonance RF absorption as a function of frequency.

a 390 gm rat are shown in Figs. 7 (*a*) and (*b*) for the 285–2000 and 2040–3840 MHz bands to illustrate the fairly small deviation between the 15 measurements. The values of the insertion loss measured for different size rats by

WAVE GUIDE LOSS W/390 GRAM RAT.
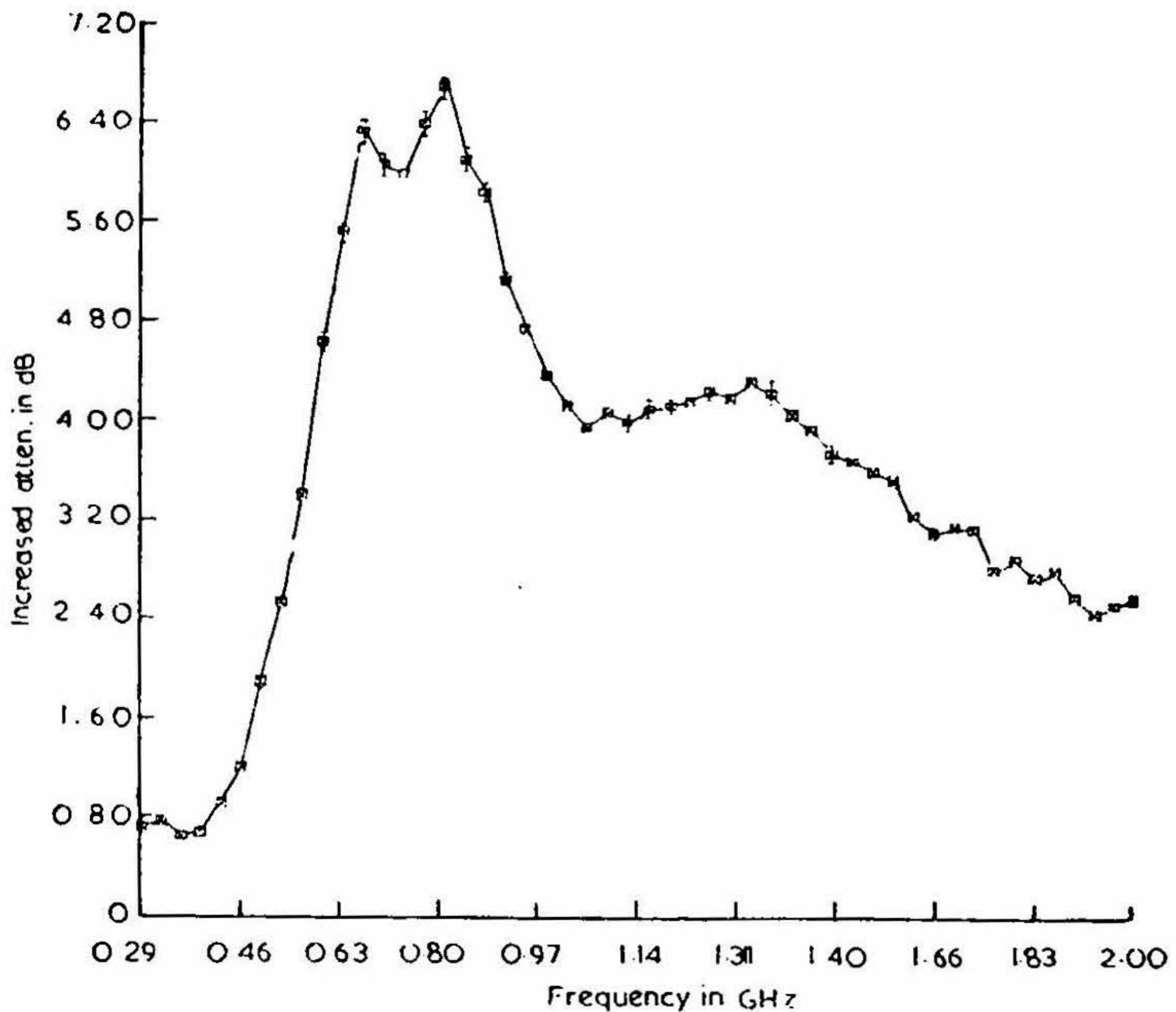
FIG. 7 (*a*). Mean value of insertion loss and standard deviation of 15 measurements for plane waves of different frequencies for a 390 gm anesthetized rat.

the two network analyzers are combined in Fig. 8. The characteristics to be noted are:

(*a*) There is a definite frequency region of peak absorption for each of the animals and the frequency for maximum absorption reduces as $W^{-1/3}$ (*see* Fig. 9) with weight W of the animal.

(*b*) For the $\hat{k} \parallel \hat{a}$ orientation of the animals, the frequencies of maximum absorption are 760, 900, 1080, and 1217 MHz for 390, 261, 158, and 96 gm rats, respectively.

(*c*) For frequencies below resonance the power absorbed (Fig. 10) varies as $f^{4.75}$ in good correlation with results on spheres, and prolate spheroids to be discussed in Section 4.

(*d*) At the absorption peak the power absorbed (Fig. 9) varies as $W^{2/3}$ with the weight of the animal. Realizing that each of the dimensions increases perhaps as $W^{1/3}$, this is tantamount to an absorption cross section proportional to the shadow cross section of the animals.

(*e*) At frequencies above resonance, the absorption reduces monotonically with increasing frequency. A larger amount of power is absorbed at 1700 MHz than that at 2450 MHz, which in turn is greater than that at 3000 MHz. The absorption measured at 1700 and 2450 MHz relative to the

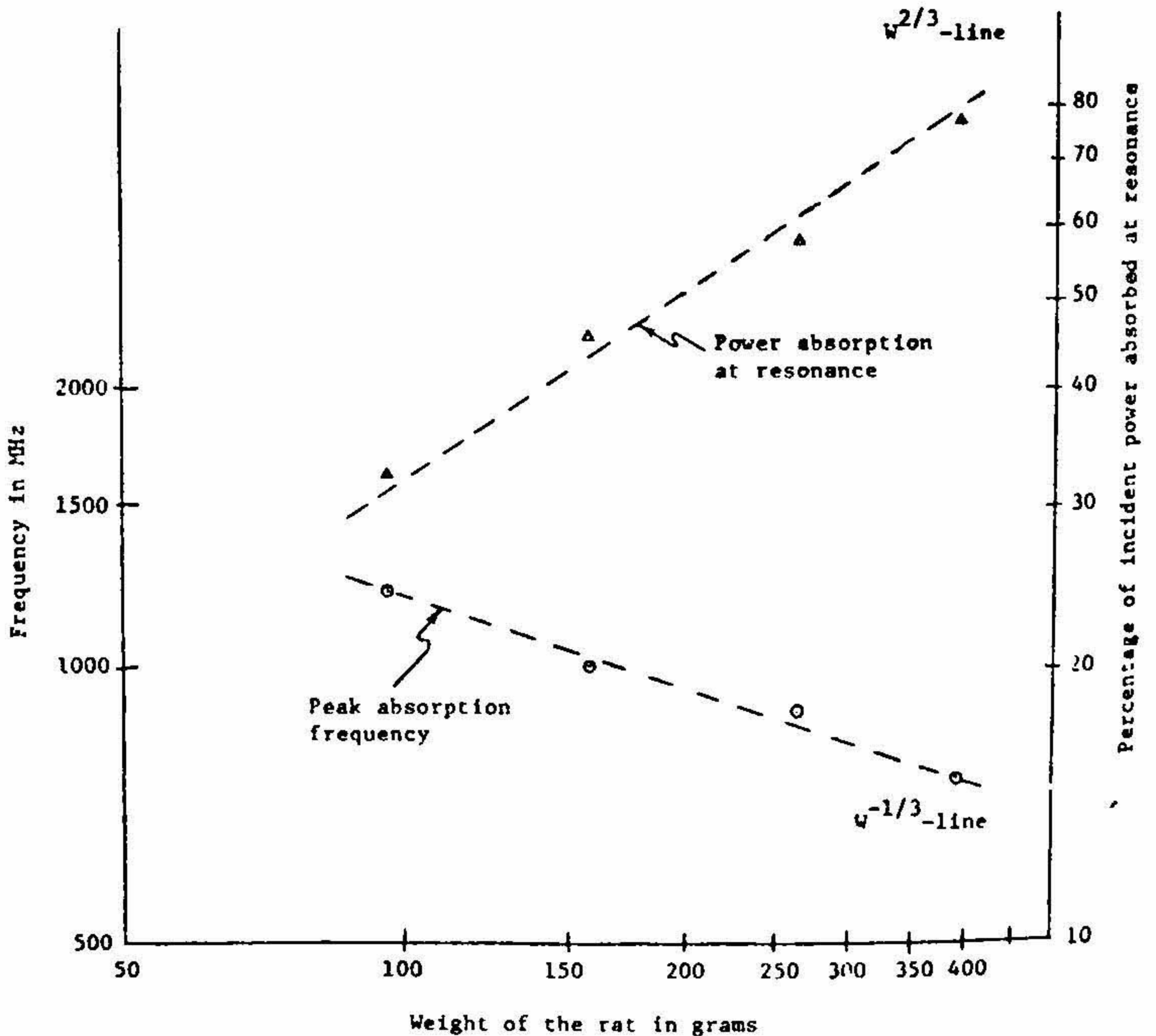Waveguide loss w/390 gram rat. ($\hat{k} \| \hat{a}$ orientation)

FIG. 7(*b*)

I. I. Sc.—2
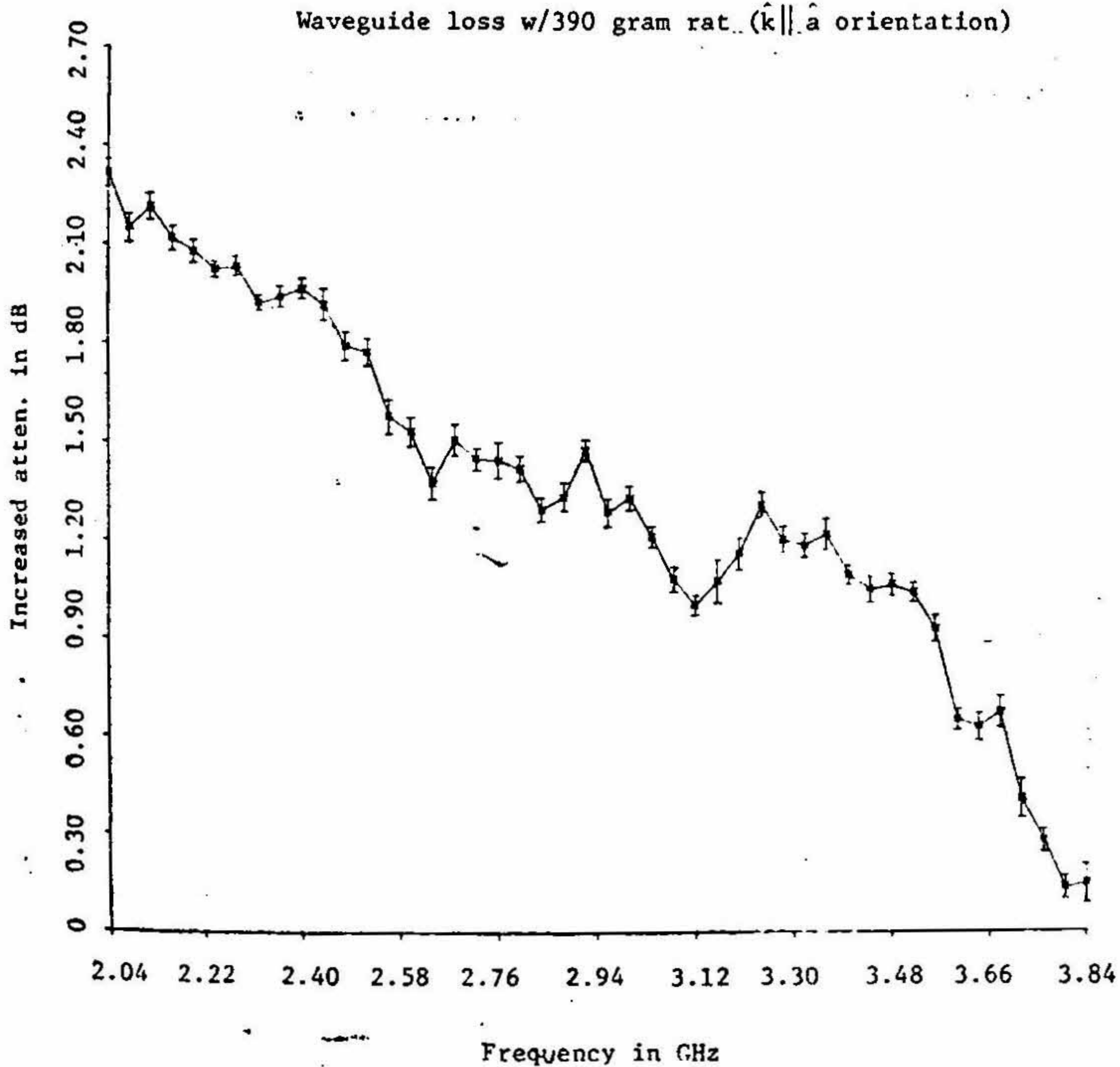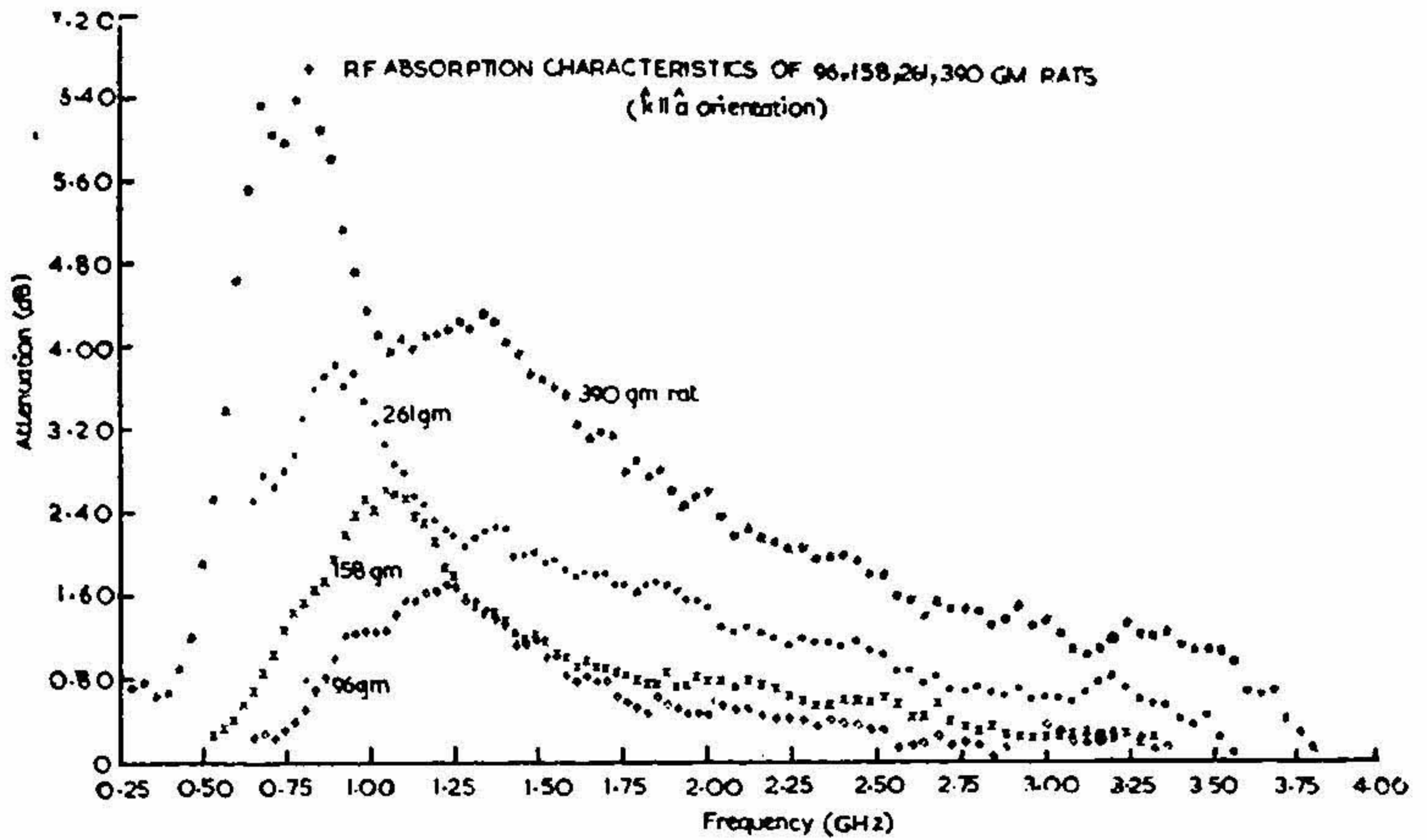
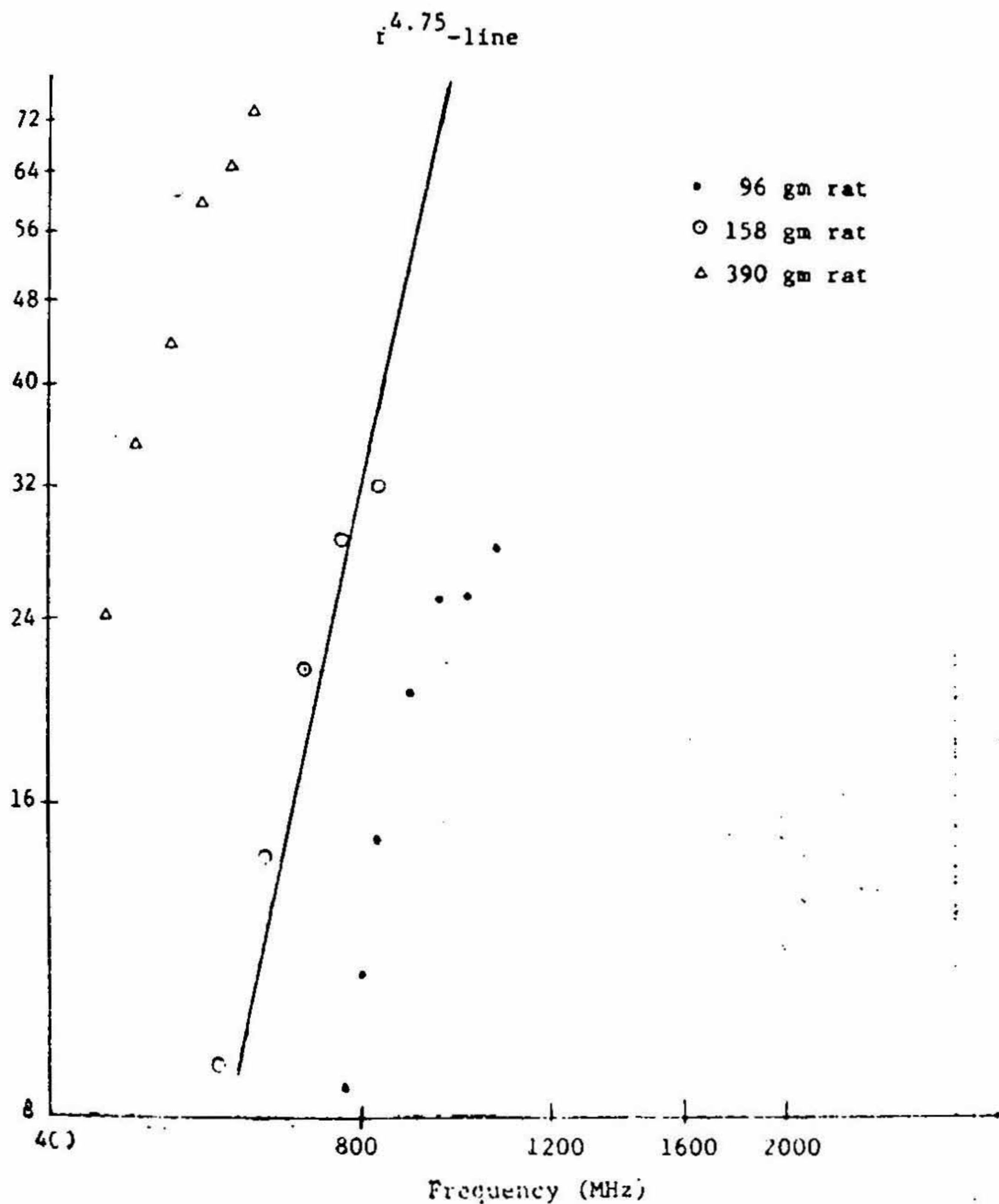FIG. 8. RF absorption for different size rats.

$r^{4.75}$-line

FIG. 10. Below resonance absorption for 96, 158 and 390 gm rats with frequency.

value at 3000 MHz is plotted in Fig. 11. Also shown in the same graph is the reciprocal of the time to work stoppage [6] relative to the value at 3000 MHz. Realizing that an increased amount of absorption may result in a reduced time to work stoppage, the correlation between the *WG* measurements and the results of the behavioral experiments can be seen to be excellent.

TABLE II

RF absorption and physical dimensional data for rats of different weights

| Weight of the Rat in Grams	Freq. of Max. Absorption MHz	Max. Insertion Loss dB	Percentage Power Absorbed	Rat Length L from Nose to Stem to Tail cm	Rat Length In Terms of Half Wavelengths	$ka = kL/2$	Measured Circumference cm	Nominal Circumference $2ab$ in cm	Aspect Ratio a/b of Equivalent Prolate Spheroid	Relative Absorption Coefficient S
96	1217	1·70	32·5	15·5	1·260	1·98	11·5 (body) max. 9·0 (head)	10·80	4·50	3·50
158	1020	2·60	45·0	18·0	1·225	1·92	13·5 (body) max. 9·0 (head)	12·82	4·30	3·33
261	900	3·80	58·3	21·0	1·260	1·98	15·0 (body) max. 10·0 (head)	15·32	4·30	3·13
390	760	6·52	77·7	23·5	1·190	1·87	18·0 (body) max. 11·0 (head)	17·70	4·35	3·13
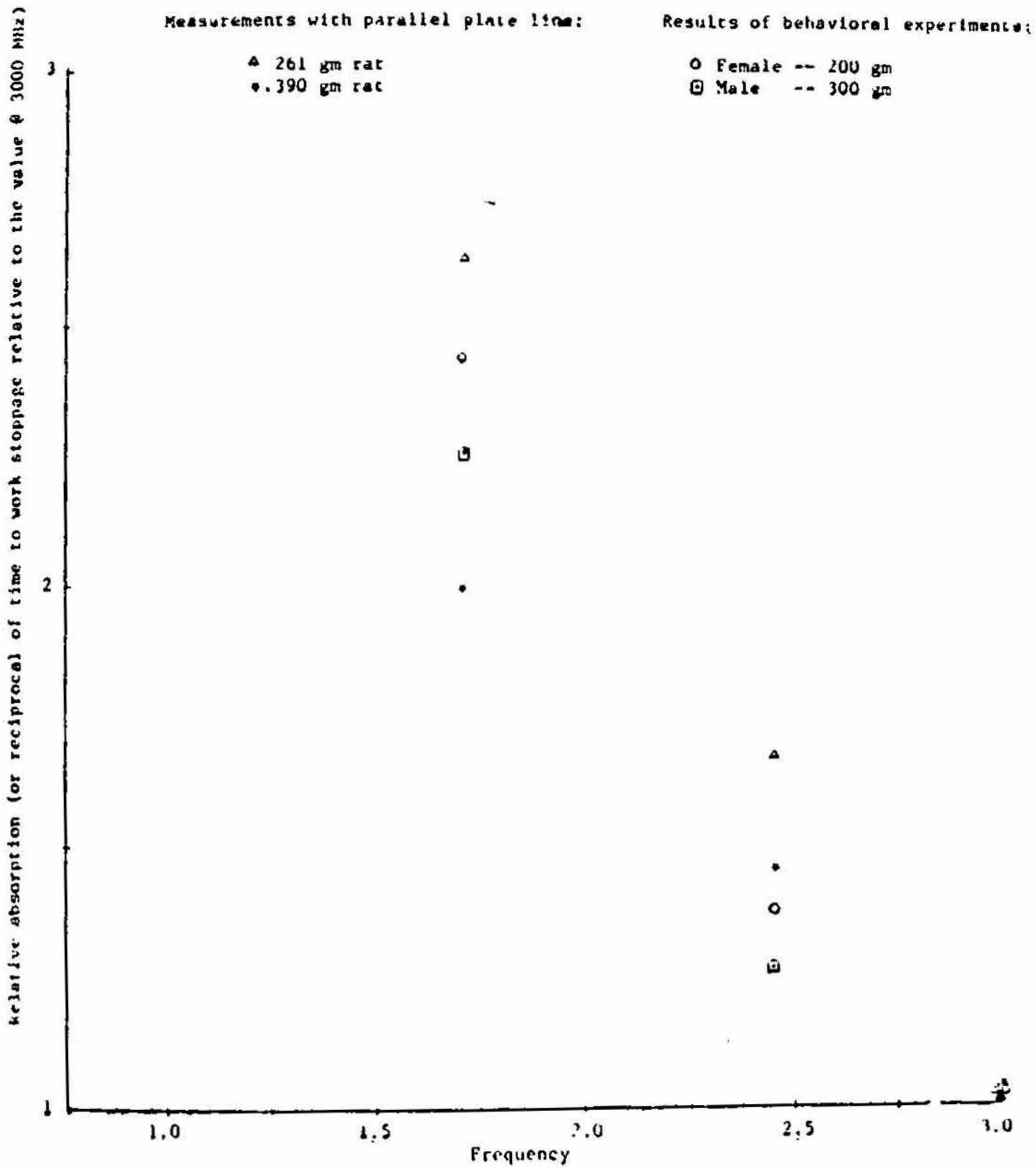
FIG. 11. Quantitative comparison of the WG measurements of power absorption with behavioral experiments on time to work stoppage.

(*f*) Absorption characteristics were identical to within 5 per cent for power incident either head-on or tail-on at the longitudinally placed animals.

(*g*) For a few animals that died due to an overdose of nembutal given to anesthetize, no discernible difference was observed for the absorption characteristics from those of the live animals for the measurements taken within minutes after demise.

(*h*) For the nonanesthetized animals placed in a polyfoam box, characteristics similar to those of anesthetized animals with the difference of a somewhat increased standard deviation ascribed primarily to the movement of the animal in the duration of the 15 measurements.

(*i*) The effect of the tail on the whole animal absorption was found to be minimal. No particular attention was therefore given to the shape/ orientation of the tail other than to ensure that it did not spill out of the *WG*.

From the foregoing, it is apparent that whole animal absorption is a size-dependent phenomenon with considerably larger *RF* absorption in certain critical frequency regions. Furthermore, the frequency of maximum absorption decreases linearly with the increased overall dimensions of the heavier rats. In order to determine the correlation of the free space wavelength at the frequency of maximum absorption with the linear dimension *L* of the animal, the body of the rat (without the tail) is approximated to an equivalent prolate spheroid. The data for the various size rats are tabulated in Table II.

In columns 2 and 3 (of Table II), the RF absorption characteristics as actually measured are listed. The frequency of peak absorption and the insertion loss thereat are read off Fig. 8. The percentage power absorbed is calculated from the data on the insertion loss. The length *L* as actually measured from the nose to the stem of the tail for each of the animals is given in column 5. The rat length in each case is on the order of $1 \cdot 19$ to $1 \cdot 26$ times the half wavelength at the frequency of maximum absorption. In the nomenclature of the equivalent prolate spheroid where $2a$ and $2b$ represent the lengths of the body along the major and minor axes, respectively, the

average value of the quantity $ka \equiv \pi f L/c$ for the rat in the $\hat{k} \| \hat{a}$ orientation is about $1 \cdot 9$. It should be recalled that the corresponding quantity for spheres was $0 \cdot 55$. Since the circumference of the rats varies a great deal, as seen from column 8, the nominal circumference of the animals for the purpose of equivalence to prolate spheroids is calculated from the expresion $2/3 \, \pi b^2 L \bar{\rho} = W$, where $\bar{\rho}$ is the average mass density. Taking $\rho = 1 \, gm \, cm^3$ (a value approximately valid for humans as well), the nominal circumference $2\pi b$ is calculated (column 9) and may be seen to correspond well to the average circumference actually measured. From the percentage power absorbed, the absorption cross section may be calculated, using the cross-sectional area of 101 cm² of the WG:

$$\text{Absorption cross section} = \frac{\text{Power absorbed}}{\text{Incident power density}}$$

$$= 101 \times \left(\begin{array}{c}\text{Power absorbed}\\\text{as a fraction of}\\\text{the incident power}\end{array}\right) \text{cm}^2 \qquad (1)$$

Dividing the effective cross section so calculated by the shadow cross-sectional area of πb^2, the relative absoption coefficient S at resonance is evaluated and is listed in Table II. This value of S of about 3·27 would be compared in the next section (Fig. 14) with the results of prolate spheroids of different a/b and seen to be consistent, too, with the measurements in free space irradiation. The similarity of ka and S for different size rats strenghtens the case for dimensional dependence of whole animal RF absorption characteristics. The value of ka of about 1·9 at resonance would also be seen in Section 4 to be reasonable when compared to the values for the $\hat{k} \| \hat{a}$-oriented prolate spheroids of lossy brain-phantom material of aspect ratios comparable to that of rats.

4. Absorption Characteristics of Lossy Prolate Spheroids

As seen in the preceding section, rats of different sizes may reasonably be approximated to prolate spheroids of aspect ratio a/b of 4·4. In this section we report on the measurements of RF absorption characteristics of lossy* prolate spheroids of aspect ratios 2, 3, 5, and 5·3. Different aspect ratios were used to develop a feel for the characteristics as they would vary for animals of various relative dimensions along the three axes. Absorption characteristics were measured, wherever possible, for $E \| a$, $k \| a$, and $\hat{H} \| \hat{a}$ orientations of the spheroid. Some representative absorption characteristics of the prolate spheroids are shown in Fig. 12. Important data for the various prolate spheroids are summarized in Table III. Important points to note are:

(a) There is considerably more absorption in the $\hat{E} \| \hat{a}$ orientation than in the other two configurations. The absorption for the $\hat{k} \| \hat{a}$ orientation is slightly larger than that for the least absorbing $\hat{H} \| \hat{a}$ configuration. This result is in qualitative agreement with the low ka theory of Ref. 5.

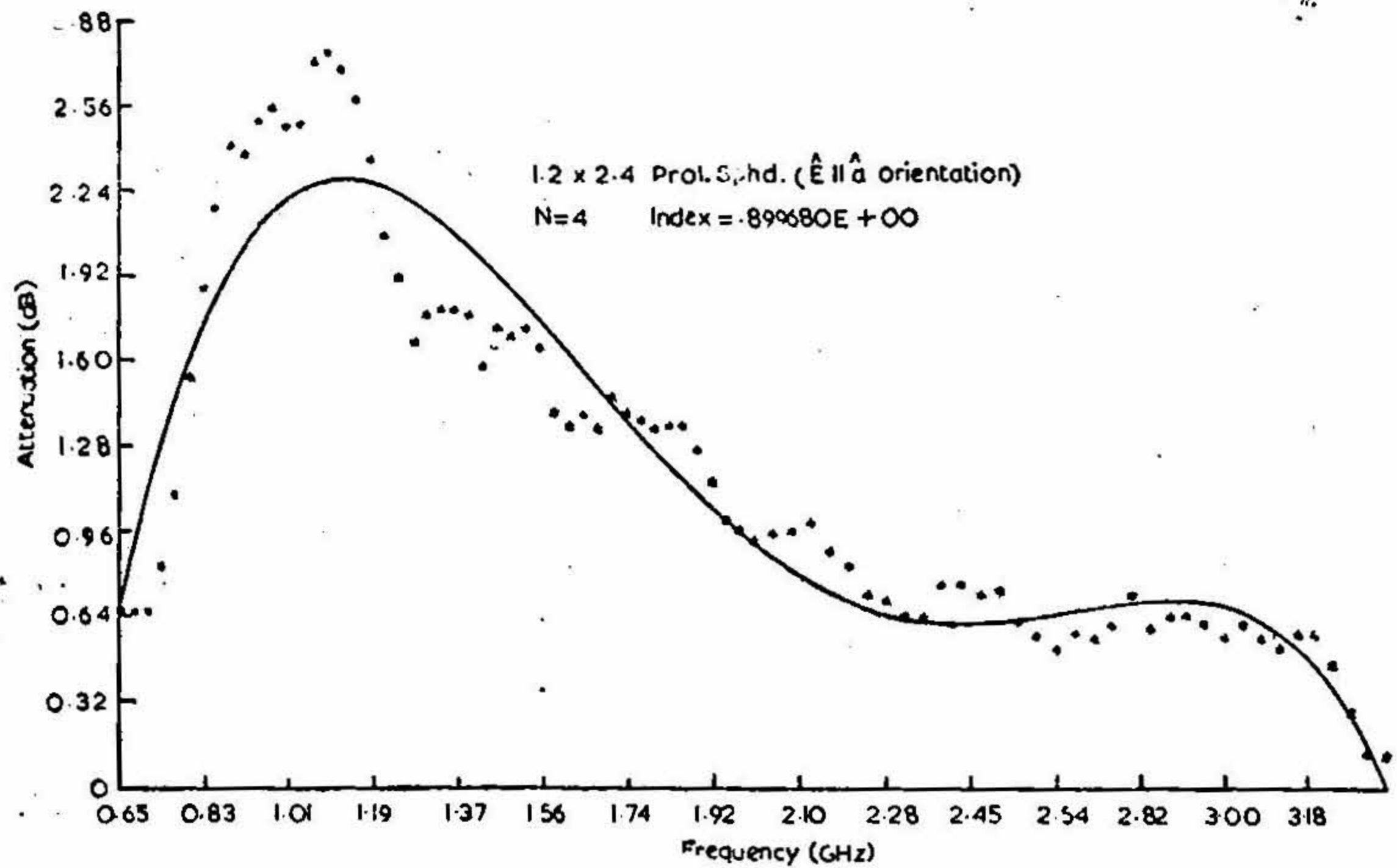* The material used was the brain-phantom material of the composition previously given.

FIG. 12 (a). RF absorption characteristics of bio logical-phantom prolate spheroids in different orientations.

[N (< 20) is the degree of the polynomial with the best fit (argerst index) and
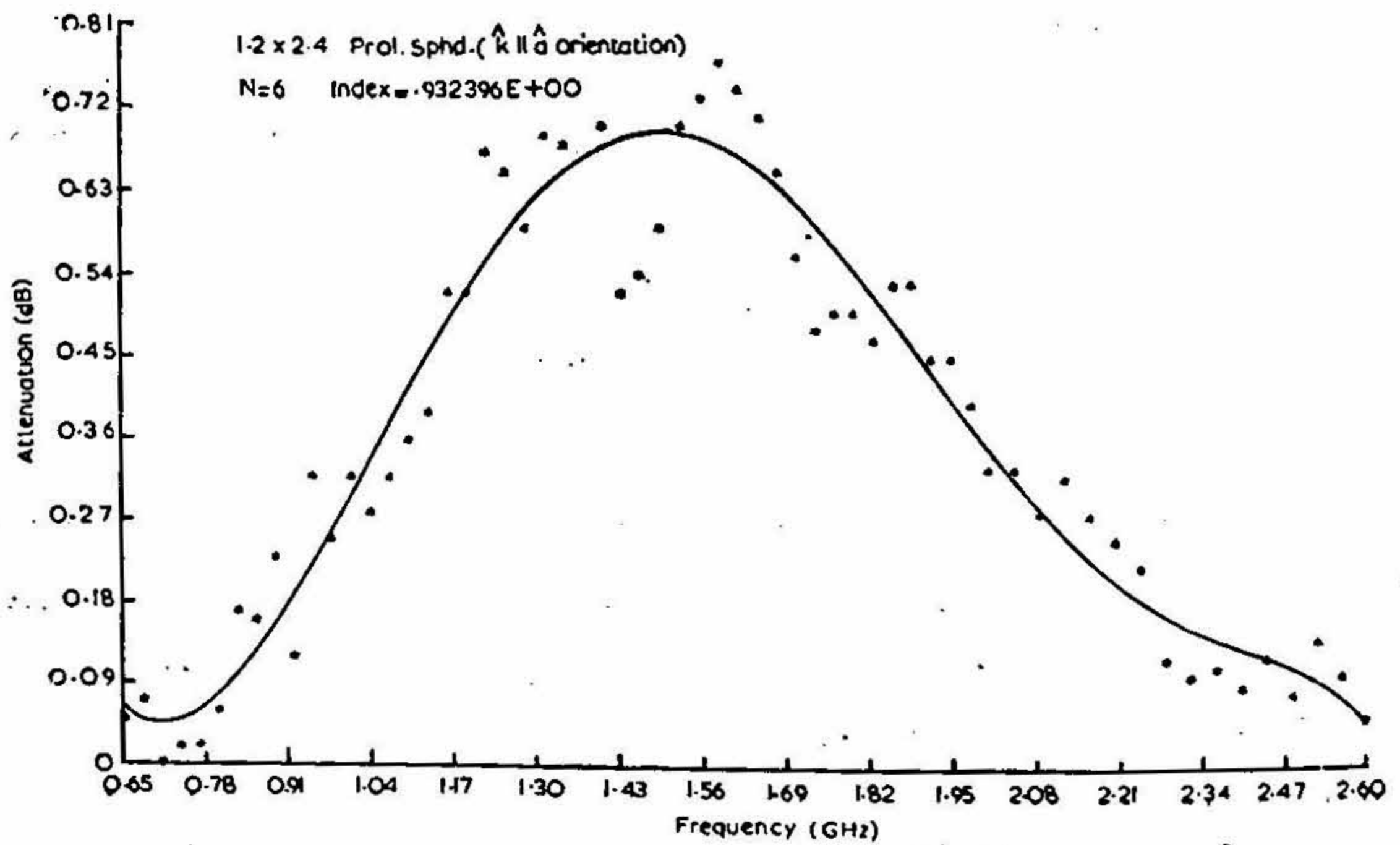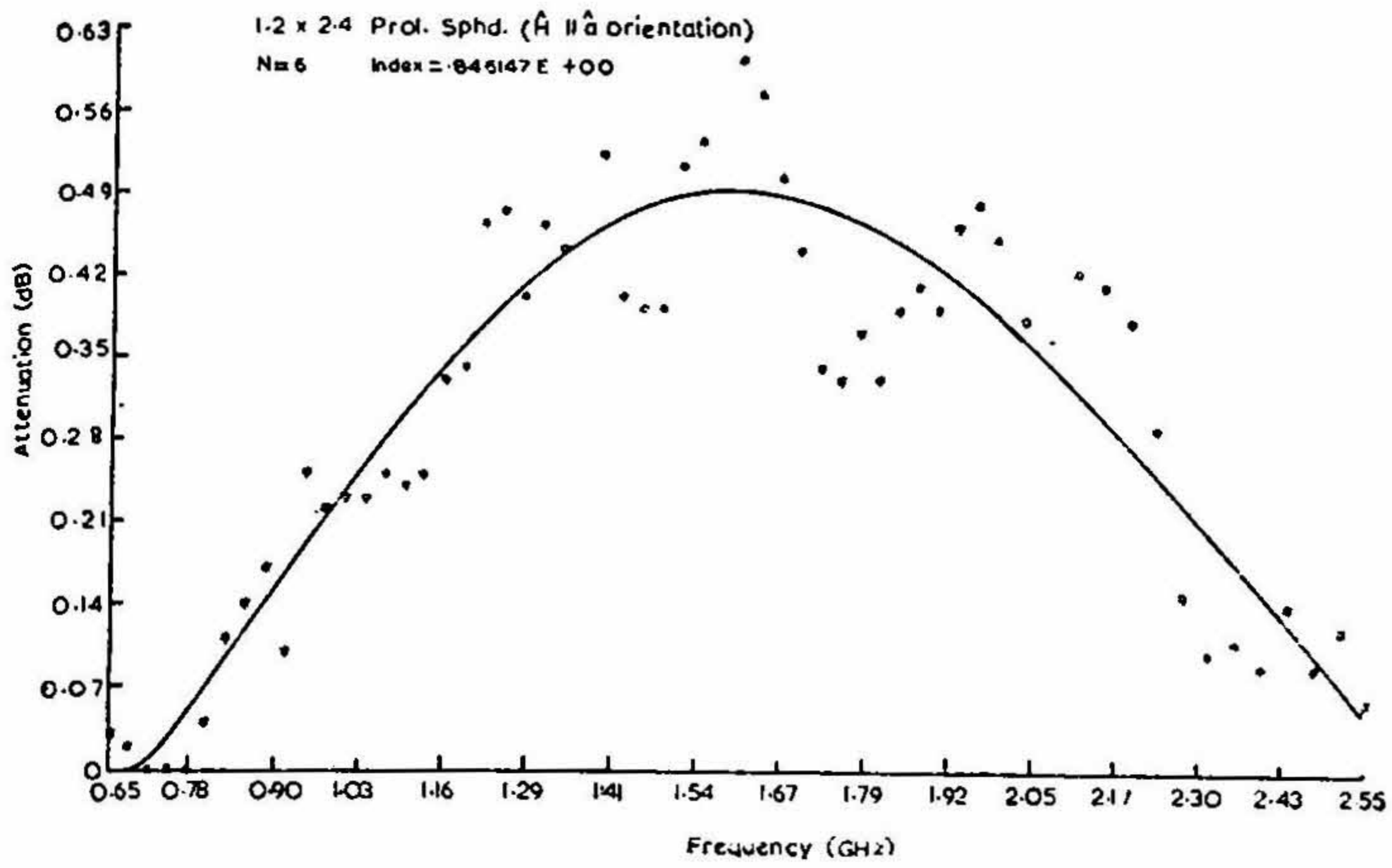Index = 1 − (Sum of the squares of the deviation from the fitted curve) / Variance]
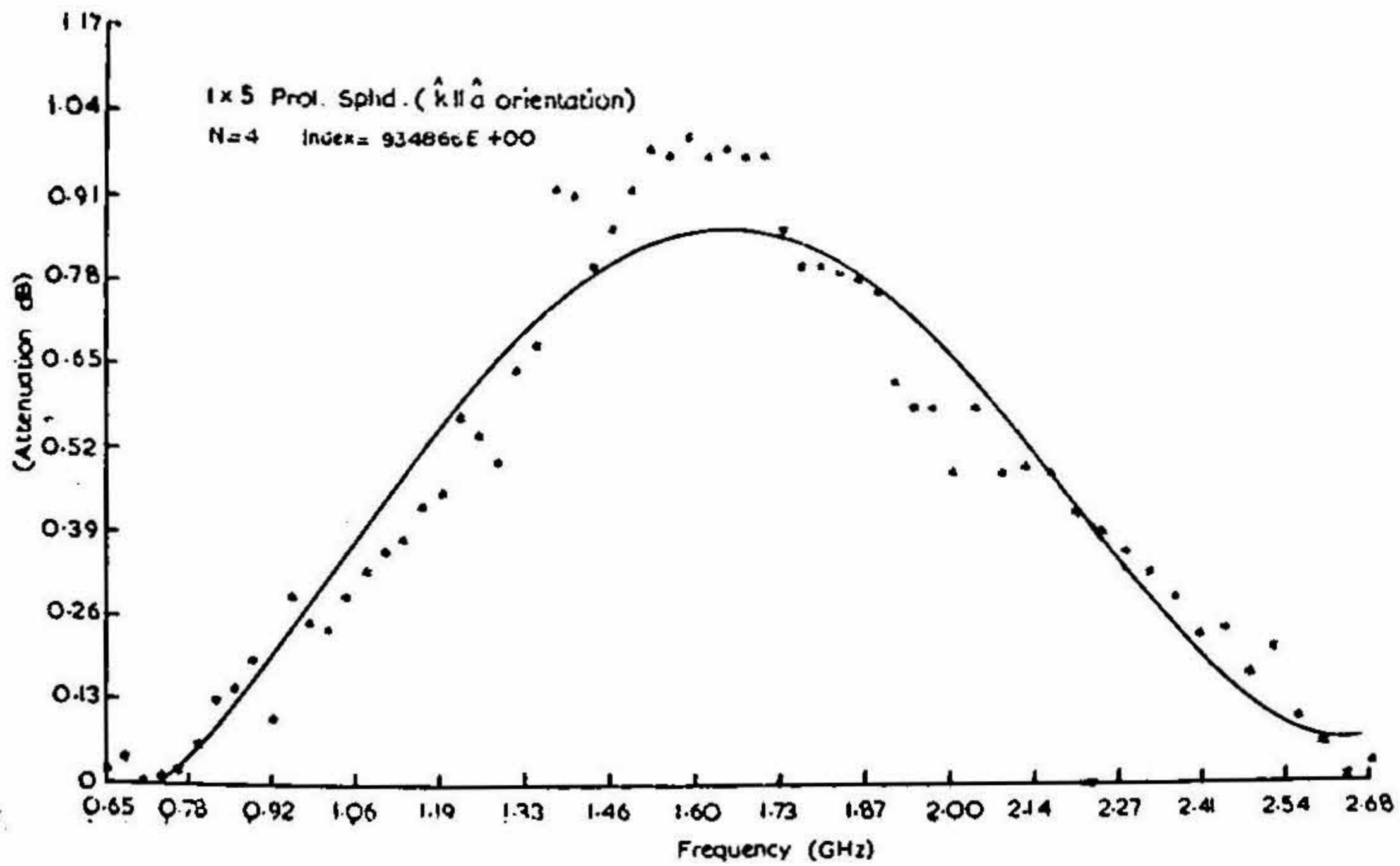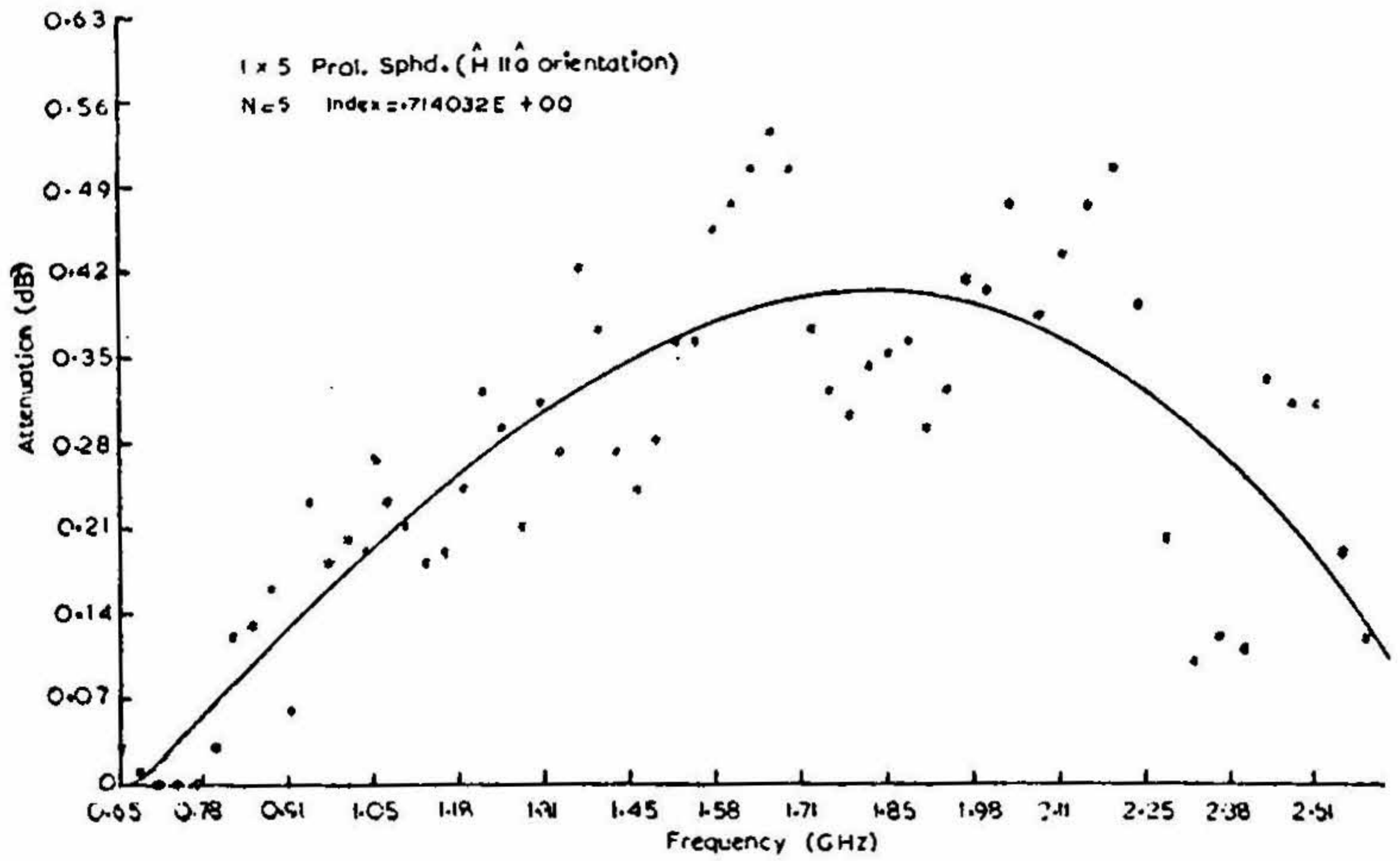
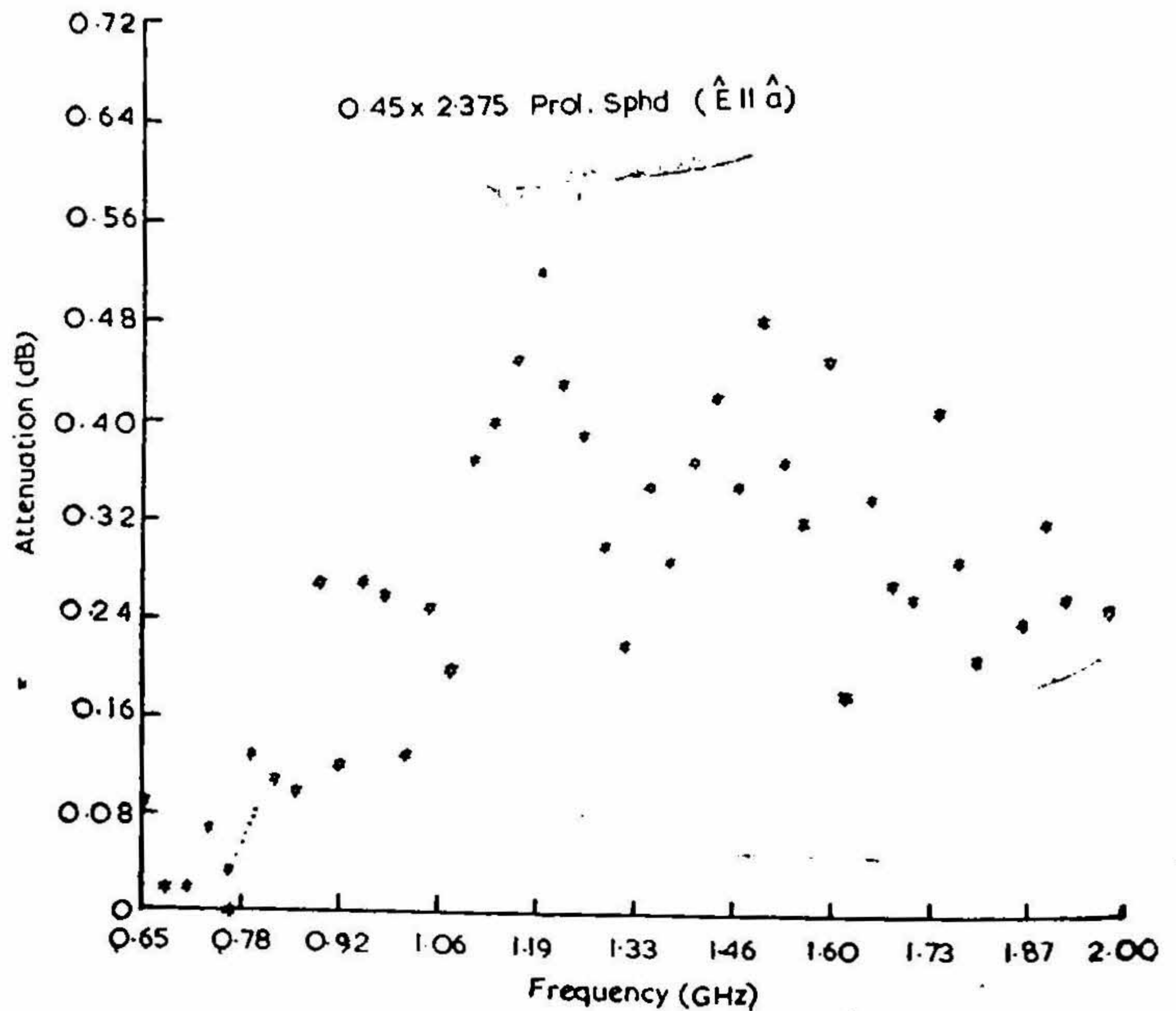

FIG. 12 (b)

Fig. 12 (c)

Fig. 12 (d)

FIG. 12 (e)

FIG. 12 (f)

Quantitative correlation with the theory is difficult because of the low ka ($\leq 0\cdot3$) validity of that analysis whereas the measurements reported here are for values of ka above $0\cdot4$ to $0\cdot5$.
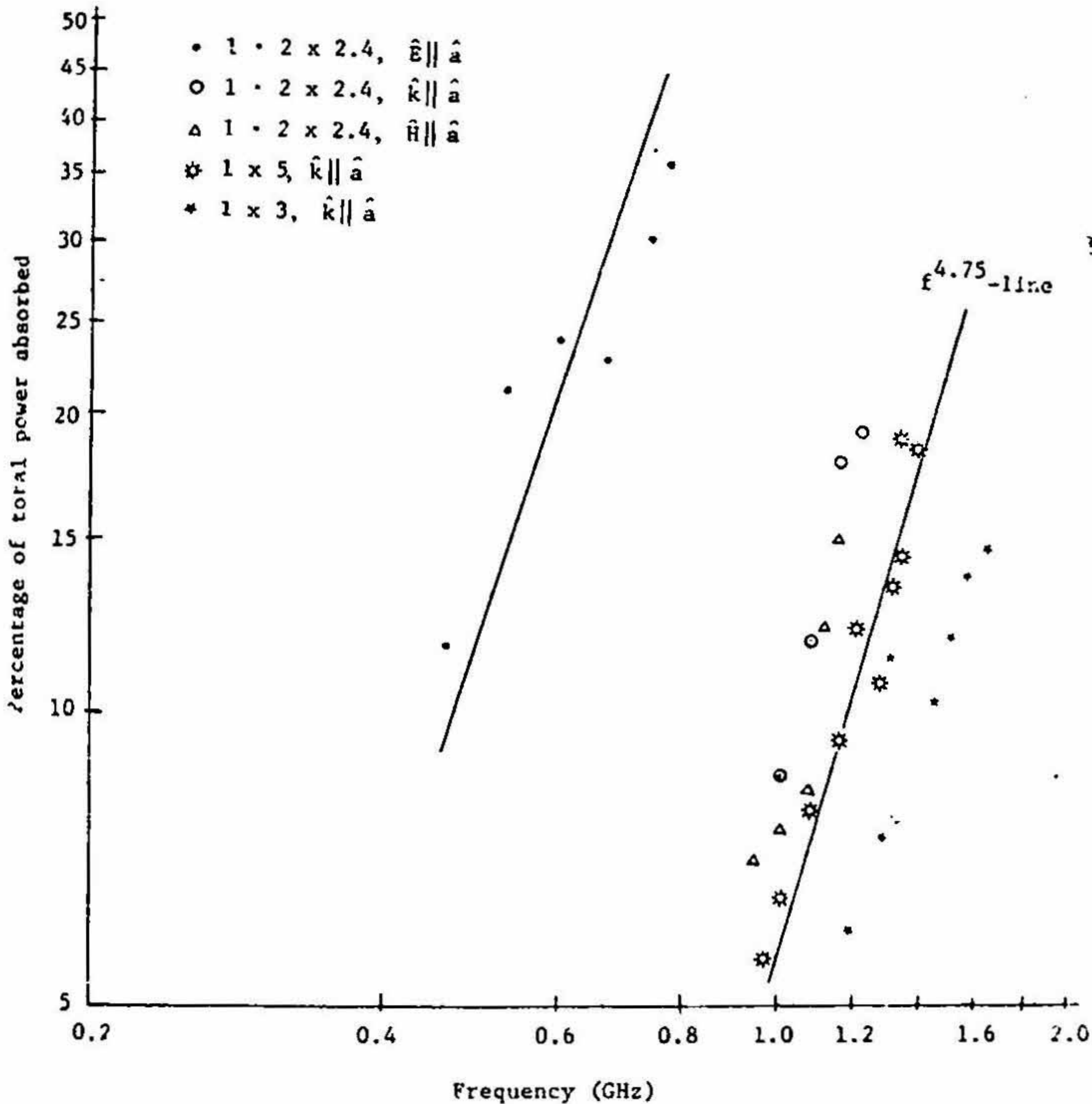

FIG. 13. Below-resonance absorption of prolate spheroids in different orientations as a function of frequency.

(b) Below-resonance absorption for prolate spheroids as a function of frequency is plotted in Fig. 13. An $f^{4\cdot75}$ dependence similar to that for spheres is observed.

(c) Even though the absorption in the $\hat{k} \parallel \hat{a}$ orientation is slightly more than that in the $\hat{H} \parallel \hat{a}$ configuration, the relative absorption coefficient S for

TABLE III

Summary of absorption characteristics for some prolate spheroids

Prolate Spheroid 2a, 2b cm	Orientation	Frequency of Maximum Absorption MHz	ka	Maximum Power Absorption Per cent	Shadow Area of the Body cm²	Relative Absorption Coefficient S
(a) 5·08, 2·54	$\hat{E} \parallel \hat{a}$	1930	1·050	14·00	10·14	1·39
	$\hat{k} \parallel \hat{a}$	2070	1·100	8·50	5·07	1·69
	$\hat{H} \parallel \hat{a}$	2150	1·145	8·00	10·14	0·80
(b) 6·0, 3·0	$\hat{E} \parallel \hat{a}$	1140	0·730	40·65	14·60	2·81
	$\hat{k} \parallel \hat{a}$	1500	0·960	15·00	7·30	2·07
	$\hat{H} \parallel \hat{a}$	1600	1·045	10·50	14·60	0·73
(c) 7·62 × 2·54	$\hat{E} \parallel \hat{a}$	Data Not Available (N/A)				
	$\hat{k} \parallel \hat{a}$	1680	1·34	12·50	5·07	2·49
	$\hat{H} \parallel \hat{a}$	1680	1·34	7·50	15·22	0·50
(d) 12·7 × 2·54	$\hat{E} \parallel \hat{a}$	N/A				
	$\hat{k} \parallel \hat{a}$	1640	2·18	18·00	5·07	3·59
	$\hat{H} \parallel \hat{a}$	1820	2·42	9·00	25·37	0·36
(e) 6·03 × 1·14	$\hat{E} \parallel \hat{a}$	1320	0·83	9·20	5·40	1·72

Bodies c and d could not be run in the $\hat{E} + \hat{a}$ orientation on account of the maximum parallel plate separation of 6·35 cm for the designed WG.

the $\hat{k} \parallel \hat{a}$ case is considerably higher. This is on account of the relatively smaller shadow area of prolate spheroids in the $\hat{k} \parallel \hat{a}$ orientation.

(*d*) The resonance frequency for $\hat{E} \| \hat{a}$ orientation is smaller than that for $\hat{k} \| \hat{a}$ resonance which in turn is smaller than that for $\hat{H} \| \hat{a}$ resonance. This is in consonance with the general sketch of Fig. 1.

(*e*) For the $\hat{E} \| \hat{a}$ configuration resonance occurs for values of *ka* on the order* of $0 \cdot 75-1 \cdot 0$ which implies that the body is approximately a quarter wavelength tall at frequencies of maximum absorption.

(*f*) For $\hat{k} \| \hat{a}$ and $\hat{H} \| \hat{a}$ configurations *ka*'s for resonance are comparable and are given approximately* by $a/2b$. For rats with an aspect ratio of approximately $4 \cdot 4$. the observed value of *ka* of about $1 \cdot 9$ seems reasonable when compared to $2 \cdot 18$ for a prolate spheroid of aspect ratio 5.

(*g*) The values of $(S)_{\hat{k} \| \hat{a}}$ for prolate spheroids of different a/b are plotted in Fig. 14. The observed value of about $3 \cdot 27$ for rats may be seen to correlate quite well with these data.

For bodies with aspect ratios on the order of 5 to 6, typical for human beings, the observations give $\hat{E} \| \hat{a}$ resonance at $ka \simeq 0 \cdot 75-1 \cdot 0$, while the regions for maximum absorption in the other two orientations correspond to $ka = 2 \cdot 5$ to $3 \cdot 0$ or frequencies approximately three times higher. Recognizing that absorption particularly in the resonance region corresponding to the $\hat{E} \| \hat{a}$ orientation may be a great deal larger by comparison with the other two orientations, it was decided to conduct alternative experiments to ascertain this important observation. In order to demonstrate resonance and the variability of total absorption with different orientations, heating of prolate spheroids of brainphantom and saline was performed in plane wave fields of 200 mW/cm² at 1700 MHz in an anechoic chamber. Since high field intensities such as those required for heating experiments are not readily available at variable frequencies, it was decided instead to use prolate spheroids of different dimensions but the same aspect ratio to get essentially the same effect. It should be recognized that this is not a true replication

---

* To the first approximation the observed values of *ka* for resonance in the different orientations are obtained by requiring that, as for sphere[12], the shortest circumference for the lossy creeping waves launched at the center of the shadow plane be $0 \cdot 5 \ \lambda$.

of the frequency effect in that the conductivity varies somewhat in that case as the frequency is altered.
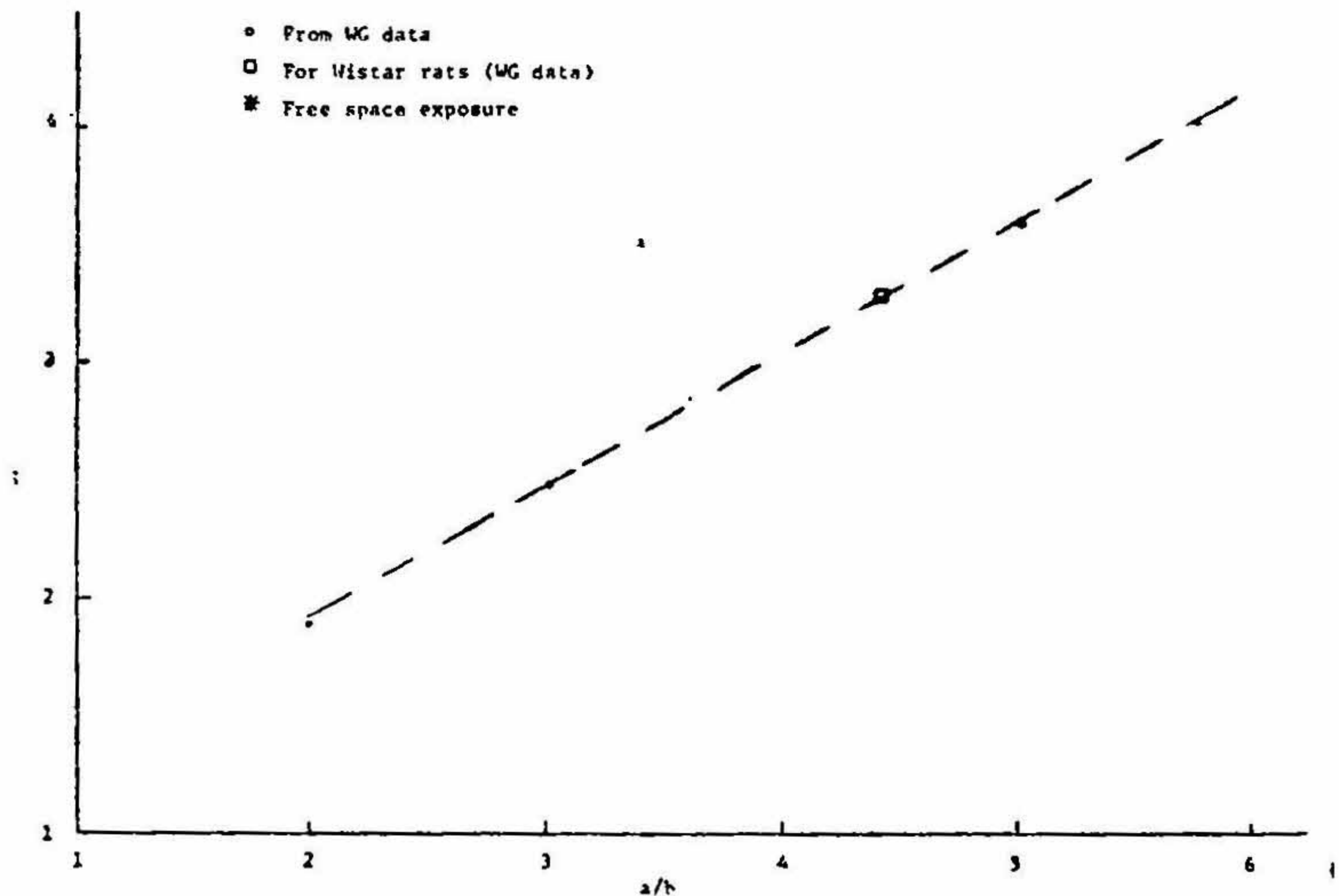

Fig. 14. Relative absorption coefficient S in the $\hat{k} \parallel \hat{a}$ orientation of prolate spheroids of different a/b.

The results of the measurements of heating per unit time of prolate spheroids filled with saline solution are plotted in Fig. 15 for six bodies. As predicted from the measurements performed on the WG, total power absorbed in the $\hat{E} \parallel \hat{a}$ configuration is considerably higher than in the $\hat{k} \parallel \hat{a}$ and $\hat{H} \parallel \hat{a}$ configurations with the former being slightly larger. Though the number of bodies used is fewer than that necessary to sketch smooth curves through the data points, the resonance phenomenon is unmistakable with twelve times larger absoption in the $\hat{E} \parallel \hat{a}$ orientation compared to the $\hat{H} \parallel \hat{a}$ configuration.

Following Anne [3] *et al.*, the heat H developed per second in the prolate spheroid may be written as

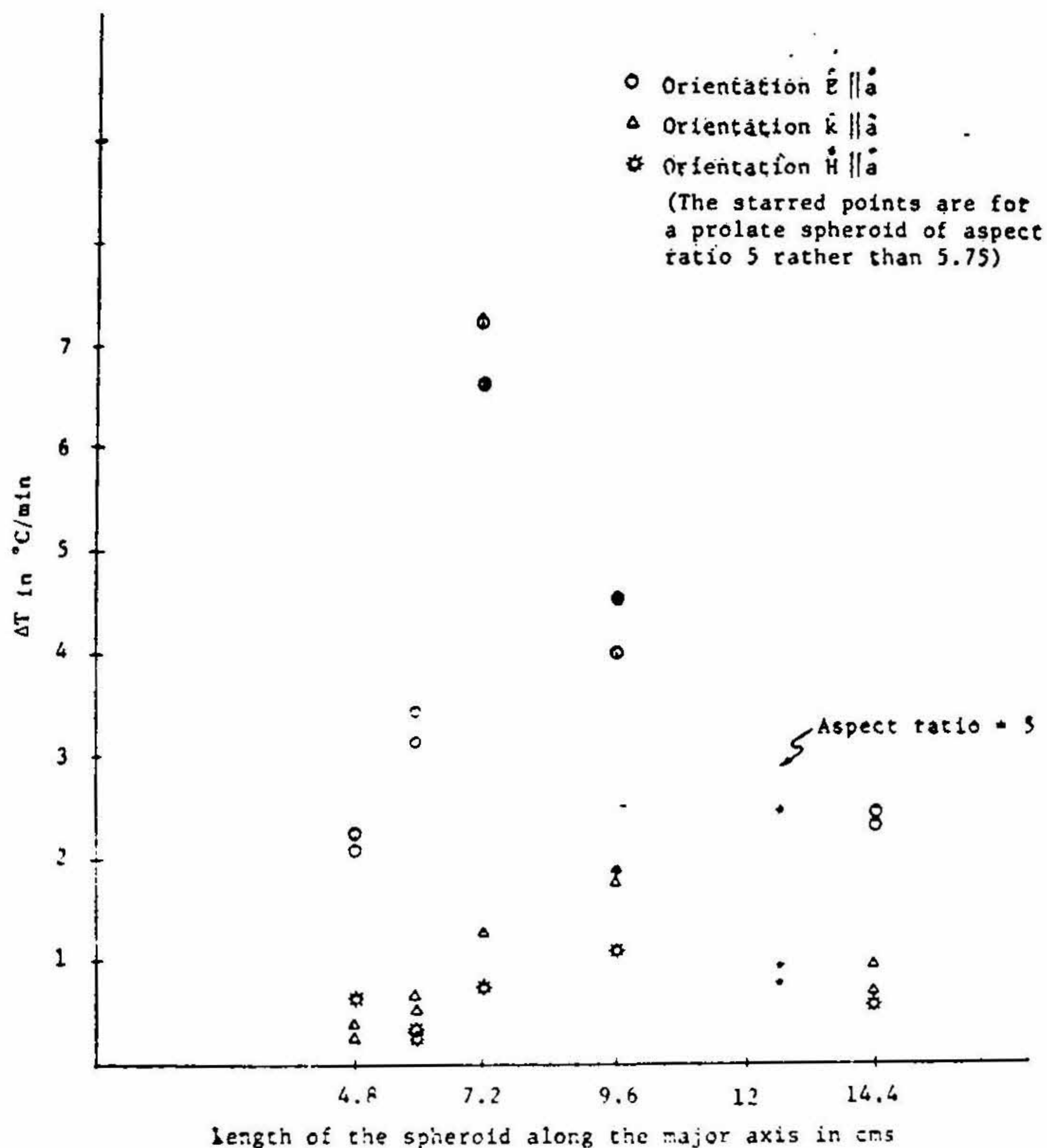$$H = 4 \cdot 2 \left(\frac{4}{3} \pi a b^2 \right) hmT \text{ watts} \tag{2}$$

FIG. 15. Plot of heating of saline for prolate spheroids of aspect ratio 5·75 in degrees centigrade/min. of exposure to microwaves of power density of 200 mW/cm² at 1700 MHz.

where

h = specific heat of the saline in calories/gm/° C

m = mass density of the saline

T = temperature rise of the saline in ° C/sec.

and a and b are the half lengths of the body along major and minor axes, respectively.

The power absorbed by the body is $P_i \times$ shadow area $\times S$ in terms of the relative absorption coefficient S and the incident power density P_i. The shadow area of the prolate spheroid is πab for $\hat{E} \parallel \hat{a}$ and $\hat{H} \parallel \hat{a}$ configurations and πb^2 for the $\hat{k} \parallel \hat{a}$ orientation.

The relative absorption coefficient therefore may be written as

$$S = \frac{5 \cdot 6 \, bhmT}{P_i} \tag{3}$$

for $\hat{E} \parallel \hat{a}$ and $\hat{H} \parallel \hat{a}$ configurations and

$$S = \frac{5 \cdot 6 \, ahmT}{P_i} \tag{4}$$

for the $\hat{k} + \hat{a}$ configuration. The relative absorption coefficients for the three orientations for the six prolate spheroids are calculated and are plotted in Fig. 16. The magnitudes of S at resonance as measured from the heating data of free space irradiation and as determined from the WG data are compared in Table IV for prolate spheroids of aspect ratio on the order of 5 to 6.

TABLE IV

Comparison of the relative absorption coefficients determined from the free space exposure and WG data

Orientation	Resonance S for Free Space Prolate Spheroids ($a/b = 5 \cdot 75$)	Resonance S from WG Measured Prolate Spheroids ($a/b = 5 \cdot 00$)
1. $\hat{E} \parallel \hat{a}$	2·02	1·72
2. $\hat{k} \parallel \hat{a}$	4·14	3·59
3. $\hat{H} \parallel \hat{a}$	0·49	0·36

An excellent correlation between the two sets of values is noteworthy. Together with the results of Fig. 14, this testifies to the viability of using a parallel plate waveguide as a simple method of determining broadband absorption characteristics of biological systems.
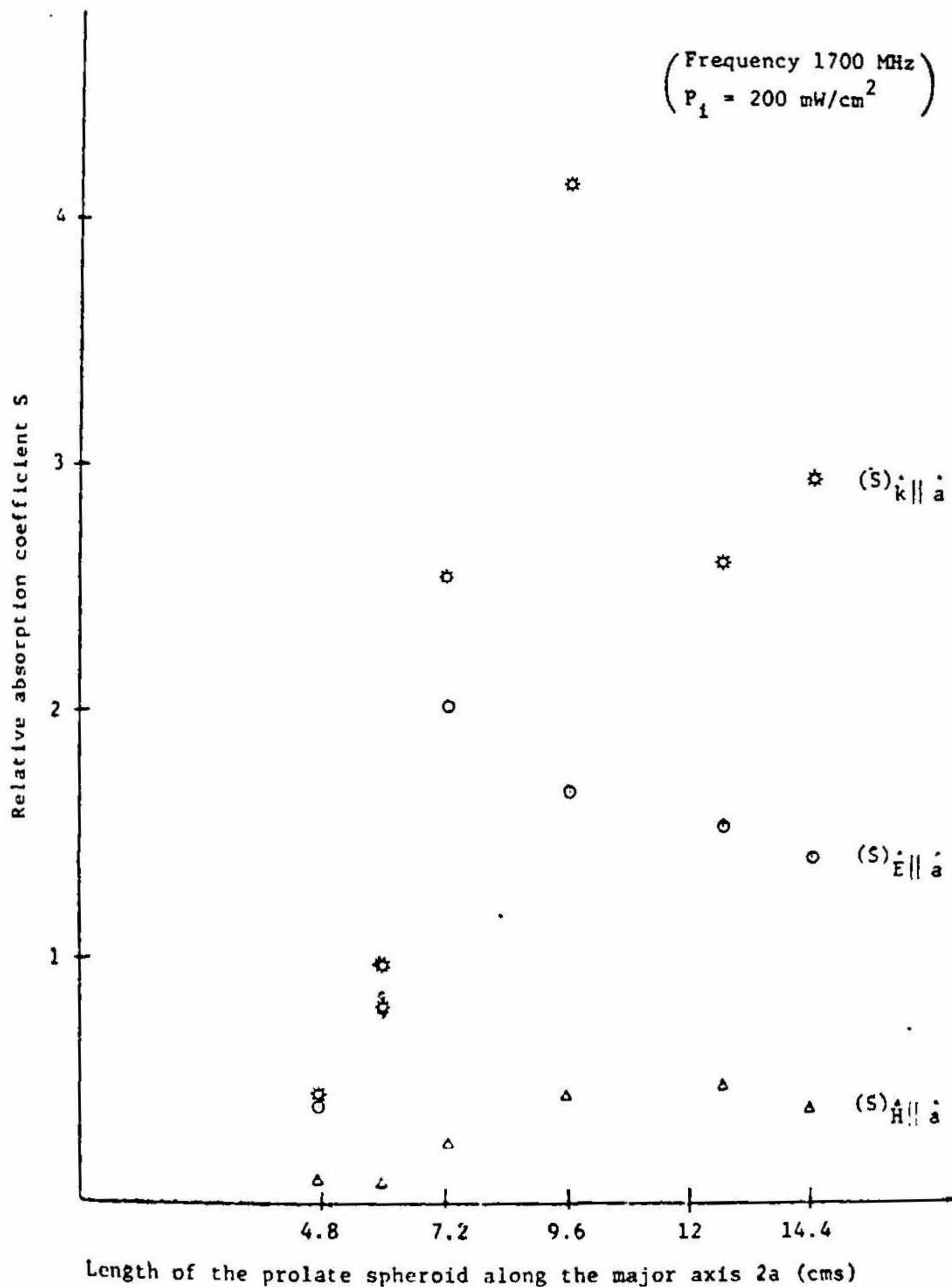
$$\left(\begin{array}{l} \text{Frequency 1700 MHz} \\ P_i = 200 \text{ mW/cm}^2 \end{array} \right)$$

$(S)_{k \parallel a}$

$(S)_{E \parallel a}$

$(S)_{H \parallel a}$

Length of the prolate spheroid along the major axis 2a (cms)

FIG. 16. Relative absorption coefficients S for the three orientations of prolate spheroids.

In further experiments prolate spheroids of brain-phantom material were heated to more closely simulate the biological bodies and also to try to compare to the results from the WG which were obtained for bodies of

I. I. Sc.—3

identical material.   The spheroids were constructed in two halves cut along
the major axis.   During the four-minute exposure to plane waves of 200mW/
cm² at 1700 MHz, the two halves were placed side by side with a separation
no more than 0·005 cm. which is clearly less than the wavelength.   Within
15–30 seconds after the exposure, the halves were separated and the tempe-
rature pattern along the major axis observed and recorded by a thermograph.
The base line or the starting temperature was recorded previous to the expo-
sure on the same photograph.   For the three prolate spheroids of aspect
ratio 5·75 corresponding to that of humans, the temperature patterns for

the $\hat{E} \parallel \hat{a}$, $\hat{k} \parallel \hat{a}$, and $\hat{H} \parallel \hat{a}$ orientations are shown in Fig. 17.   The tremendous

disparity in the amount of heating between the $\hat{E} \parallel \hat{a}$ and the $\hat{H} \parallel \hat{a}$ configu-
rations is once again dramatized.   While the thermographic method has the
advantage of giving the temperature distribution, integration for total heat
(power absorbed) is difficult and this is obtained more readily in the previously
described experiments with saline solution.

— $\hat{E} \parallel \hat{a}$ orientation

— $\hat{k} \parallel \hat{a}$ orientation

— $\hat{H} \parallel \hat{a}$ orientation;
    also base line
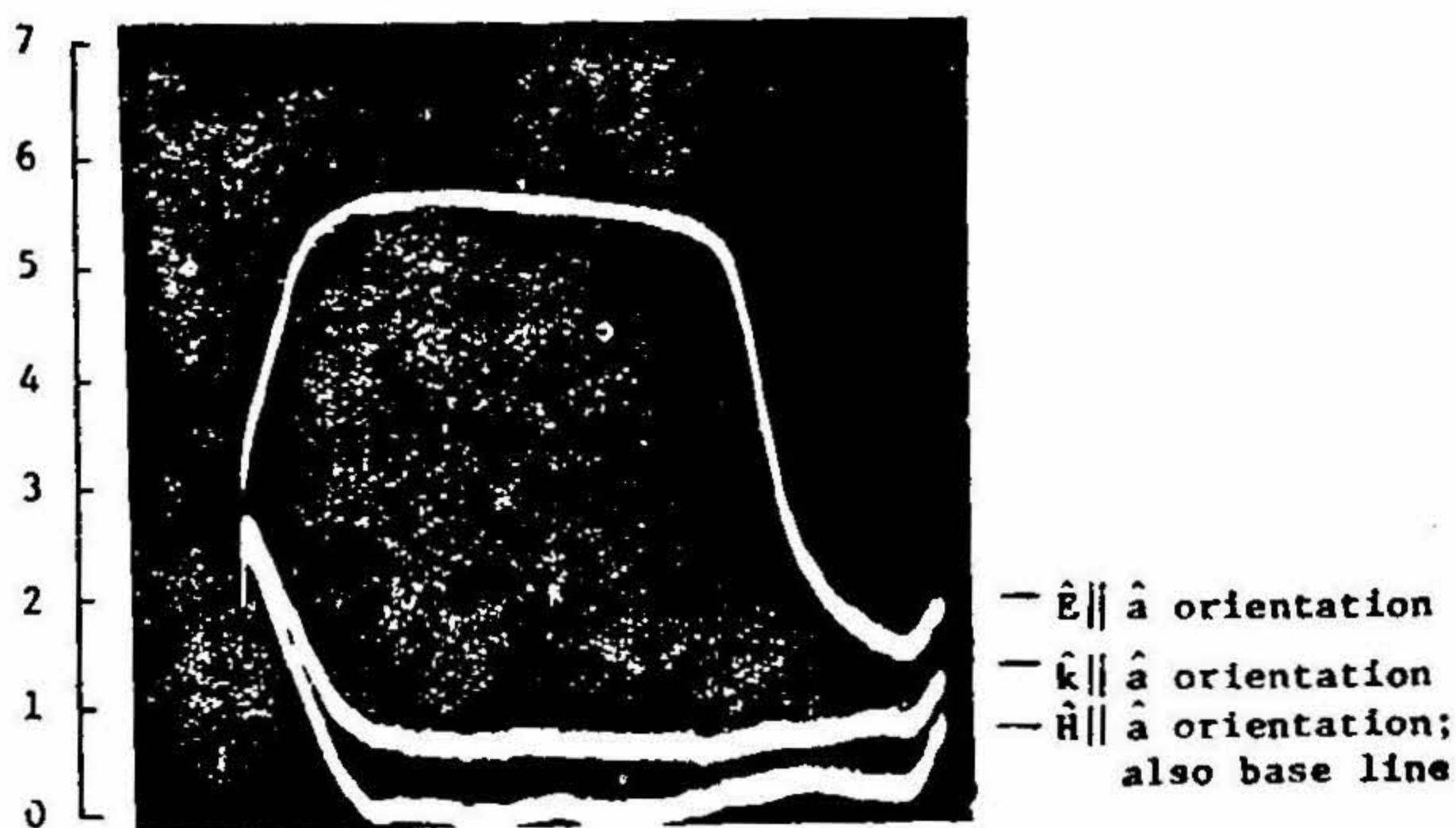
Vertical scale = 1 cm = 1·5°C

FIG. 17. Thermograms of the major axis of biological phantom prolate spheroids of
aspect ratio a/b of 5·75 (corresponding to humans); heating done by plane waves of frequency
1700 MHz; intensity 200 mW/cm²; exposure time 4 minutes.

FIG. 17 (a). $a = 2·4$ cm; $b = 0·42$ cm prolate spheroid.

Noting that an order of magnitude or more RF absorption can occur

in the biological systems in the $\hat{E} \parallel \hat{a}$ orientation for frequencies corresponding
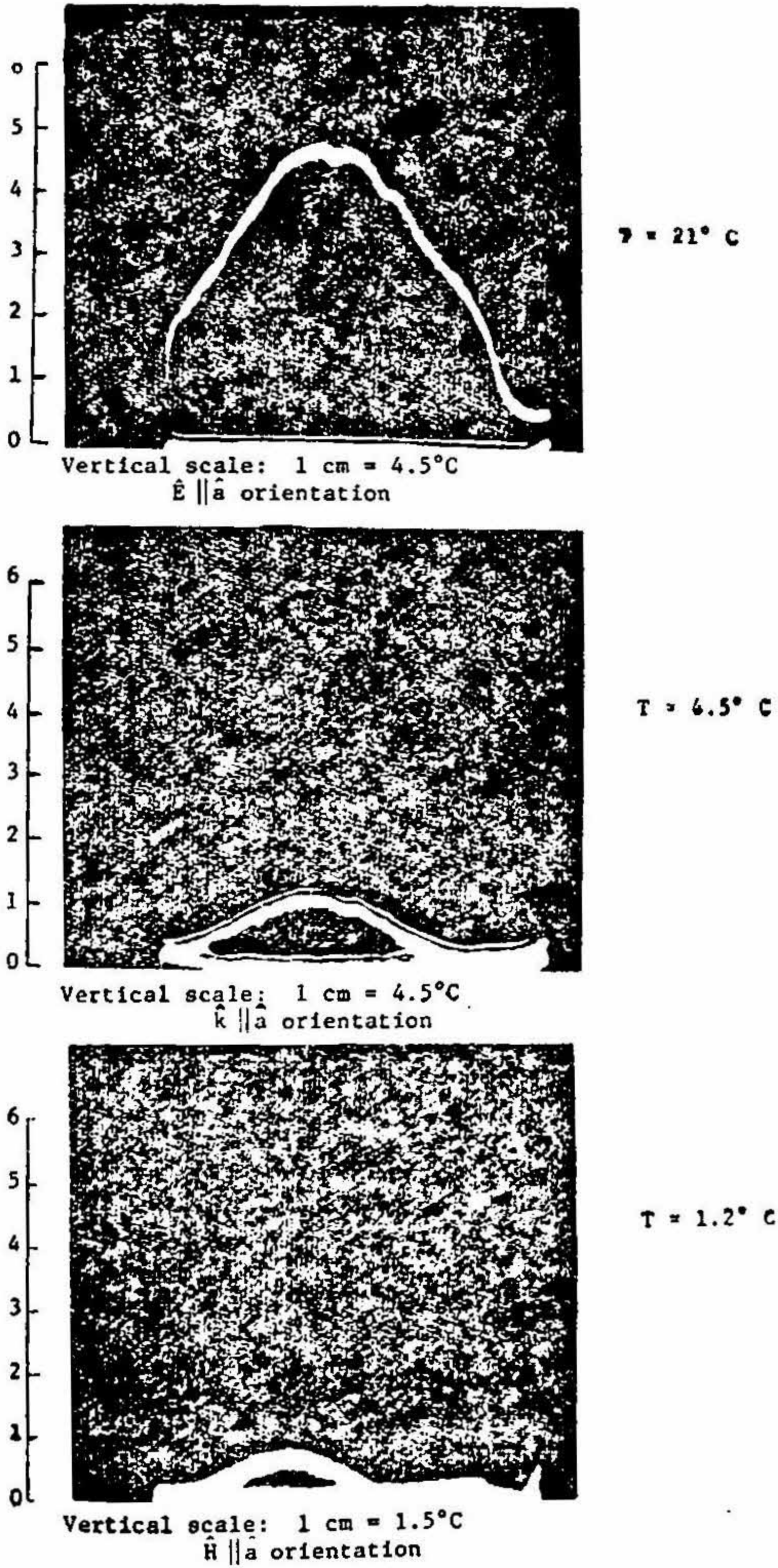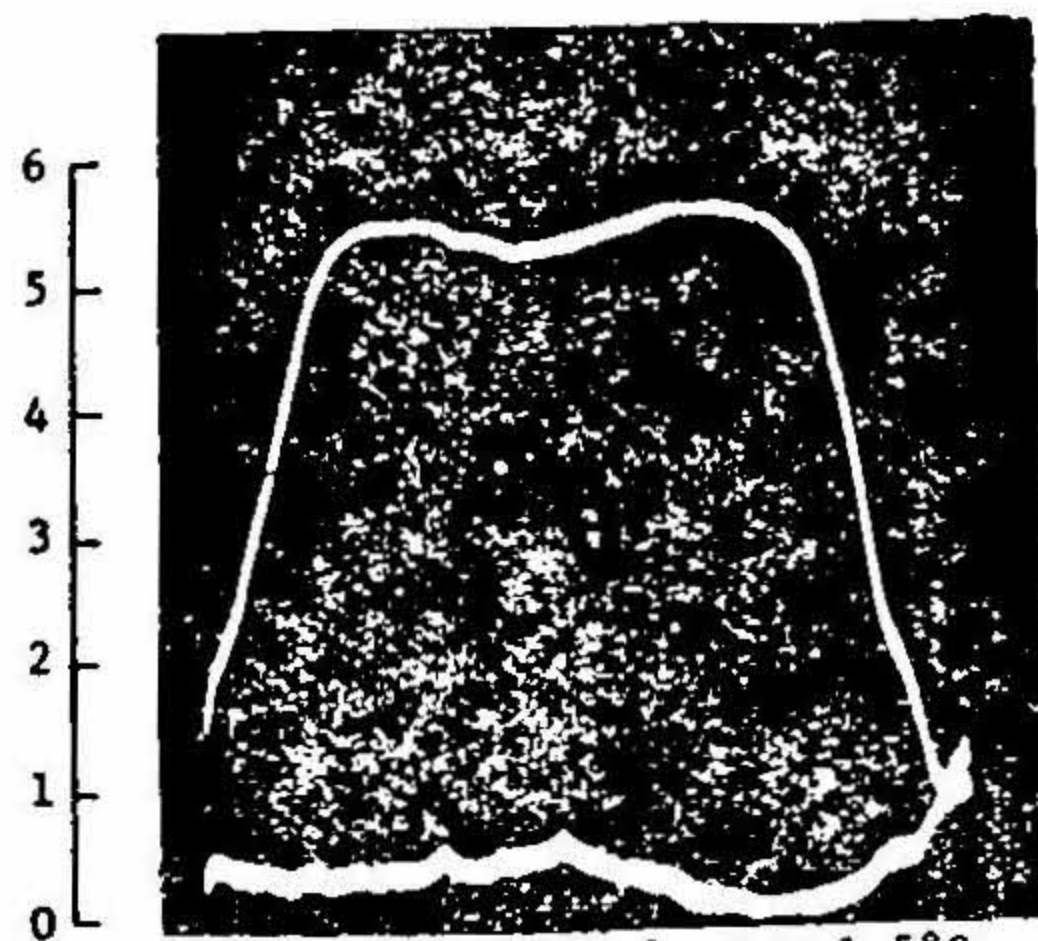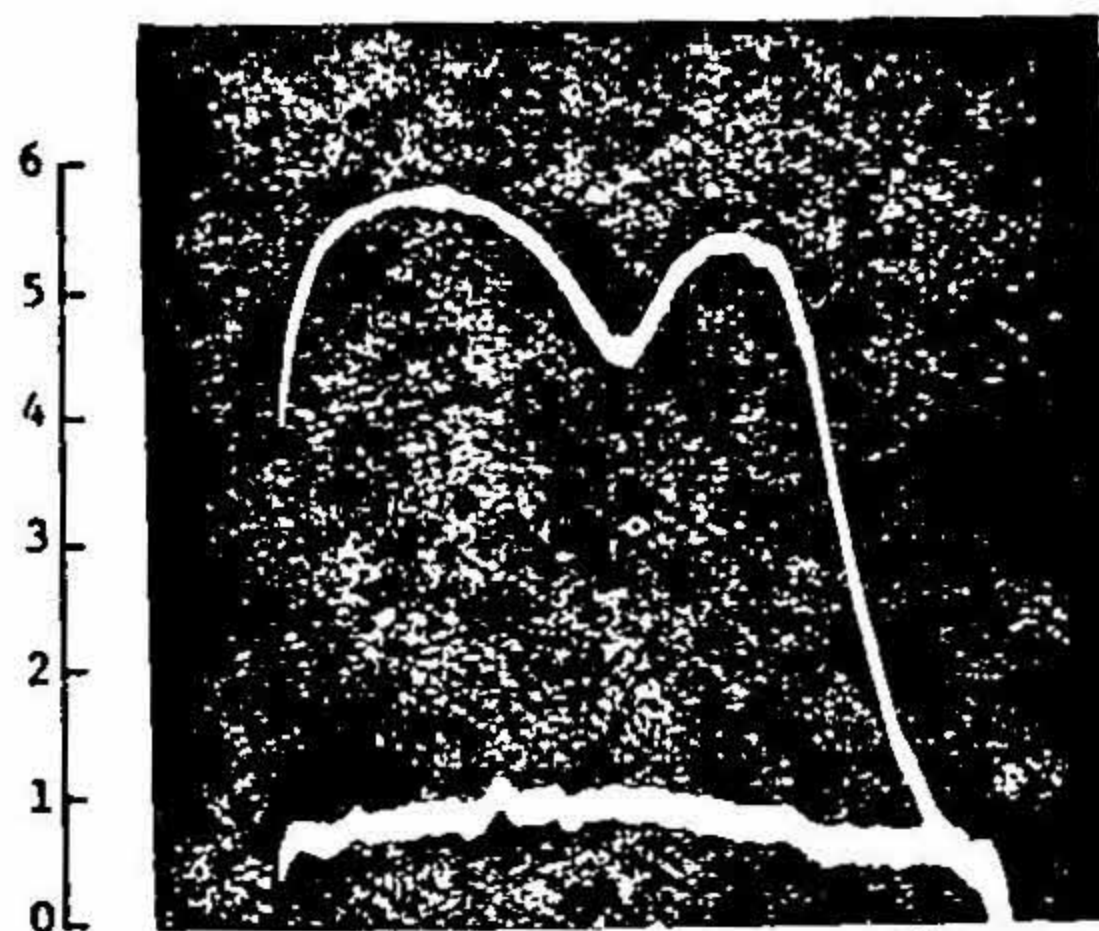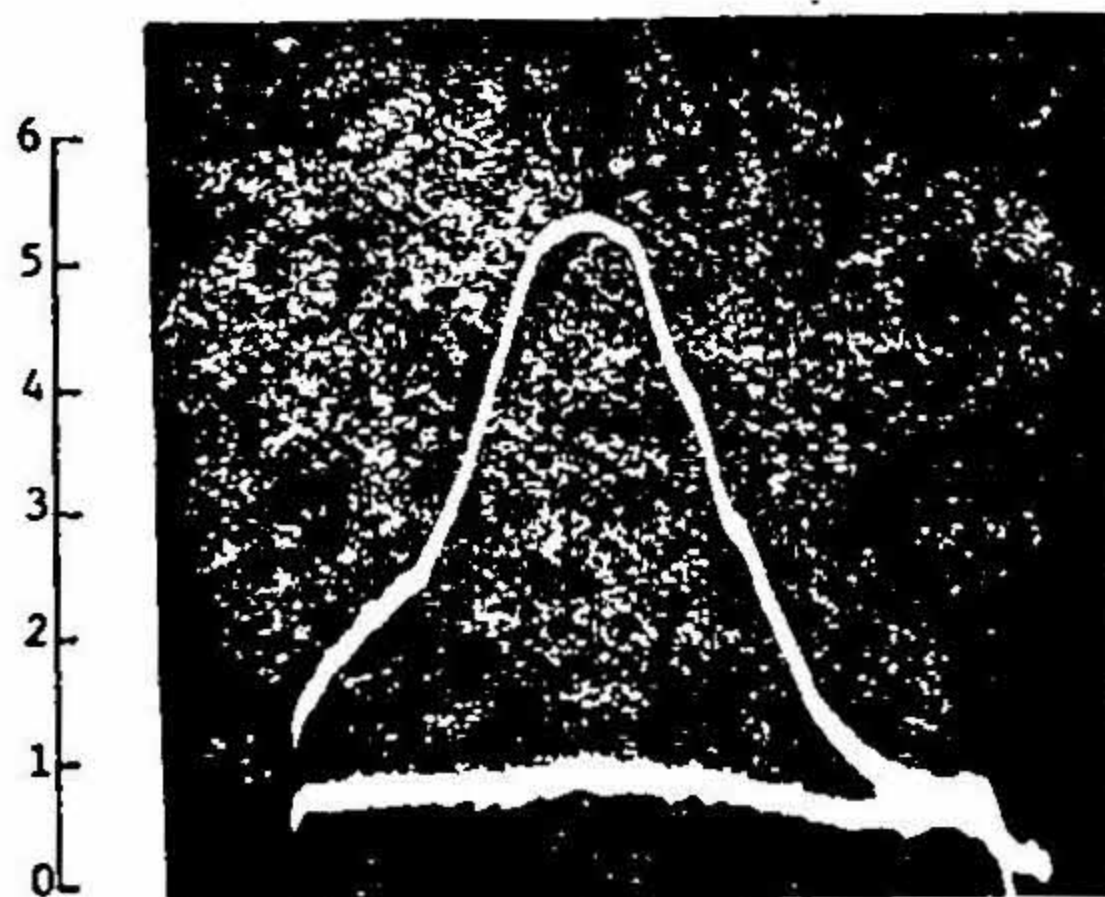to resonance than in other orientations, resulting perhaps in an increased

Vertical scale: 1 cm = 4.5°C
Ê ∥ â orientation

$T = 21°$ C

Vertical scale: 1 cm = 4.5°C
k̂ ∥ â orientation

$T = 4.5°$ C

Vertical scale: 1 cm = 1.5°C
Ĥ ∥ â orientation

$T = 1.2°$ C

FiG 17 (b). $a = 4·8$ cm; $b = 0·84$ cm prolate spheroid.

Vertical scale: 1 cm = 1.5°C
$\hat{E} \| \hat{a}$ orientation

Vertical scale: 1 cm = 1.5°C
$\hat{k} \| \hat{a}$ orientation

Vertical scale: 1 cm = 1.5°C
$\hat{H} \| \hat{a}$ orientation

FIG. 17 (c). $a = 7 \cdot 2$ cm; $b = 1 \cdot 26$ cm prolate spheroid.

hazard, a case must be made for the need to account for the frequency and orientations effects in microwave biological effects research.

5. ABSORPTION CHARACTERISTICS OF PARALLELEPIPED SHAPED BODIES

In order to recognize the different dimensions of biological bodies along the three axes, it may be worthwhile to represent the bodies as ellipsoids rather than spheroids. In actual measurements, because of its fabrication simplicity, a rectangular parallelepiped (dimensions $2 \cdot 5 \times 3 \cdot 8 \times 5 \cdot 7$ cm^3) of brain-phantom material was instead used to obtain a feeling for the orientational effects on the RF absorption of such bodies. The characteristics as actually measured are shown in Fig. 18. The main results are summarized in Table V. The configuration with $\vec{E}$ and $\vec{H}$ along the longest and shortest
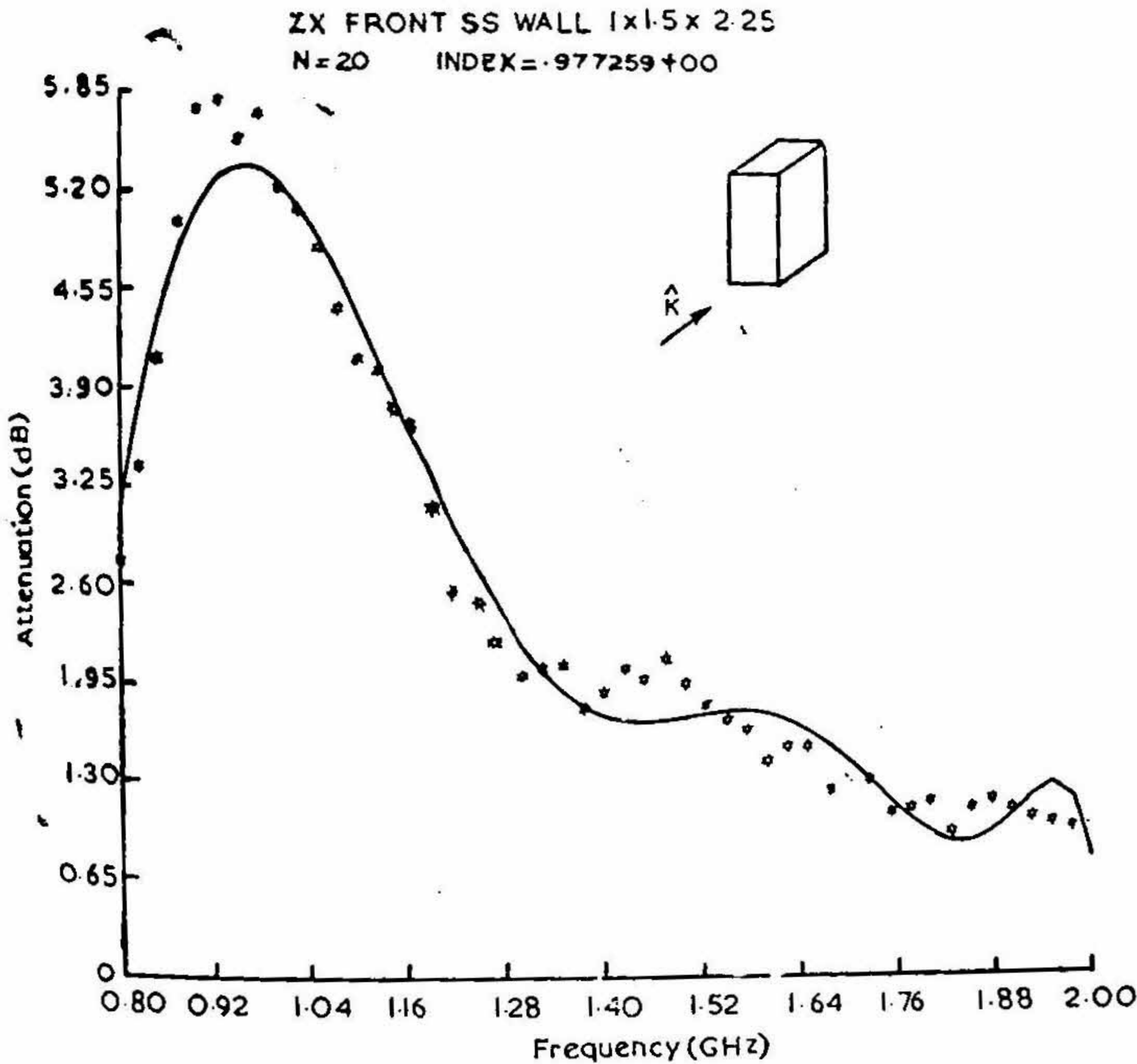
FIG. 18 (*a*). RF absorption characteristics of a rectangular parallelepiped of dimensions $1 \times 1 \cdot 5 \times 2 \cdot 25$ inch^3 in the six facial orientations to plane waves.

dimensions, respectively, is the most absorbing orientation. For $\hat{k} \parallel \hat{a}$ and $\hat{H} \parallel \hat{a}$ configurations, a larger amount of power is absorbed if $\vec{E}$ is along the intermediate dimension than if it is along the smallest dimension.
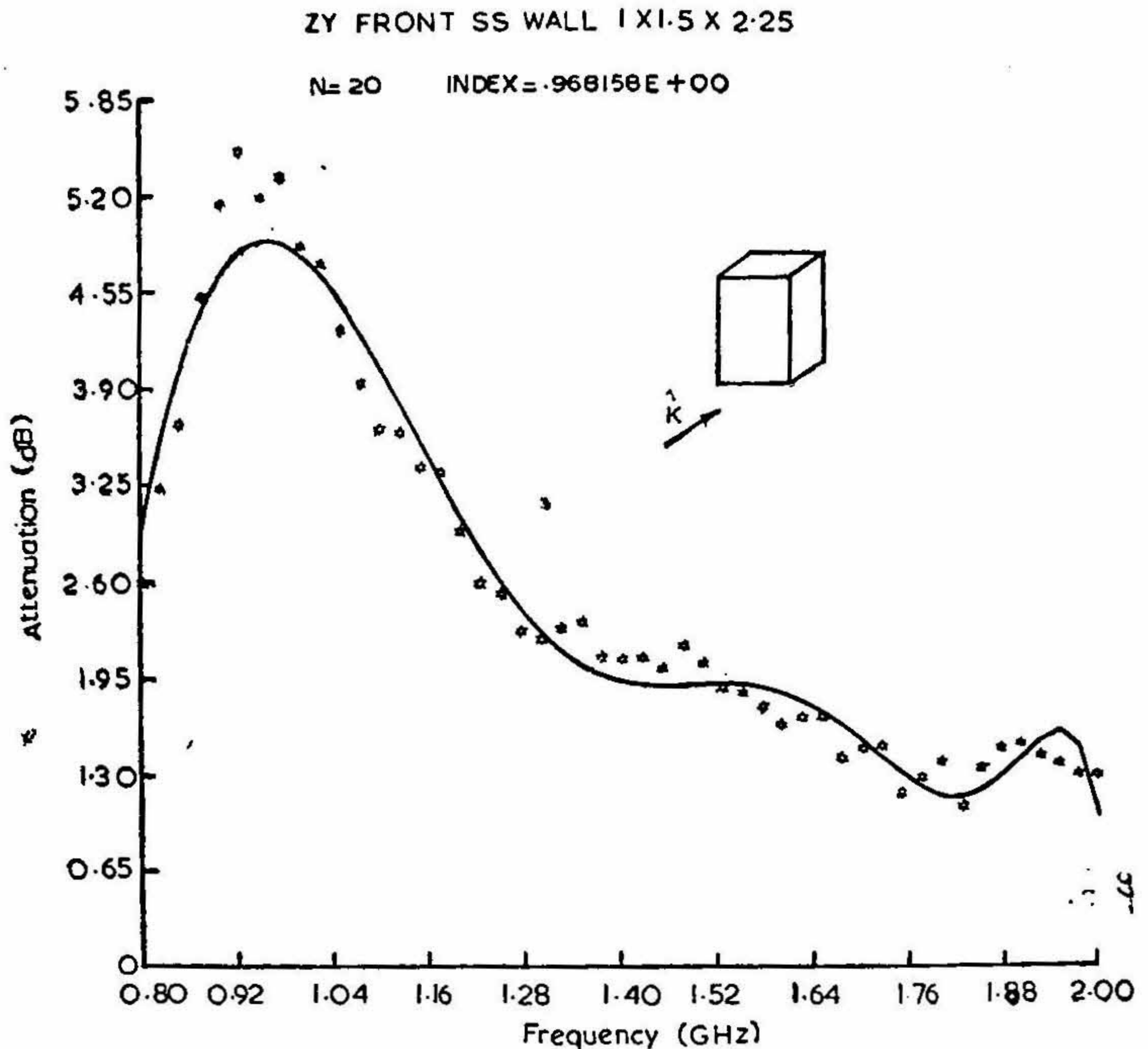
ZY FRONT SS WALL I X I·5 X 2·25

N= 20   INDEX = ·968I58E +OO

Fig. 18 (b)

It should be noted in conclusion that several parallelepipeds of different aspect ratios or perhaps ellipsoids need to be studied to completely understand the orientational/frequency effects of such bodies.

6. MODELLING OF BIOLOGICAL SYSTEMS BY PHANTOMS

To check on the validity of modelling of biological systems by brain-phantom bodies to the first approximation, two full scale models of 165 gm

and 390 gm rats were sculptured and measured for RF absorption in the WG. Their characteristics are given in Fig. 19. The similarity to the RF absoption characteristics of anesthetized rats is remarkable. This strengthens the previously mentioned observation that whole animal absorption is a size-dependent phenomenon with a definite region for peak absorption.
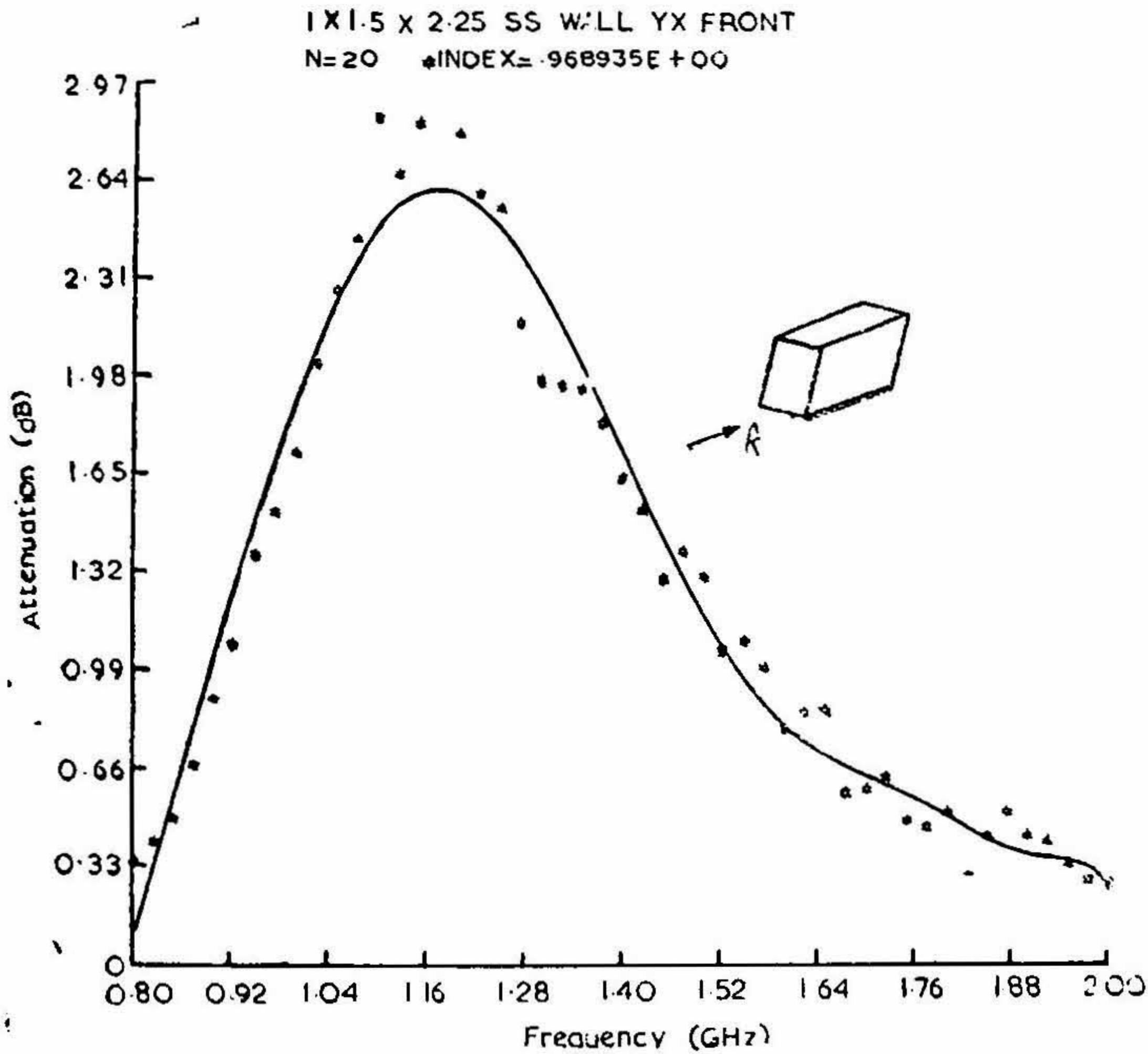

FIG. 18(c)

7. POWER ABSORPTION BY 25 gm MOUSE IN THE THREE ORIENTATIONS

As seen from the experiments on prolate spheroids, the highest absorption peaking at the smallest frequency occurs for the vertical orientation. For the $6 \cdot 35 \times 15 \cdot 9$ cm² cross-sectional dimensions of the WG, the only orientation feasible with rats is $\hat{k} + \hat{a}$, and this was used for the results reported in Section 3. To substantiate the orientational and frequency effects for

a whole animal, a 25 gm mouse was measured for total power absorption in the three orientations. The results of the measurements are given in Fig. 20 and bear out the main features of the orientational/frequency effects observed with prolate spheroids.
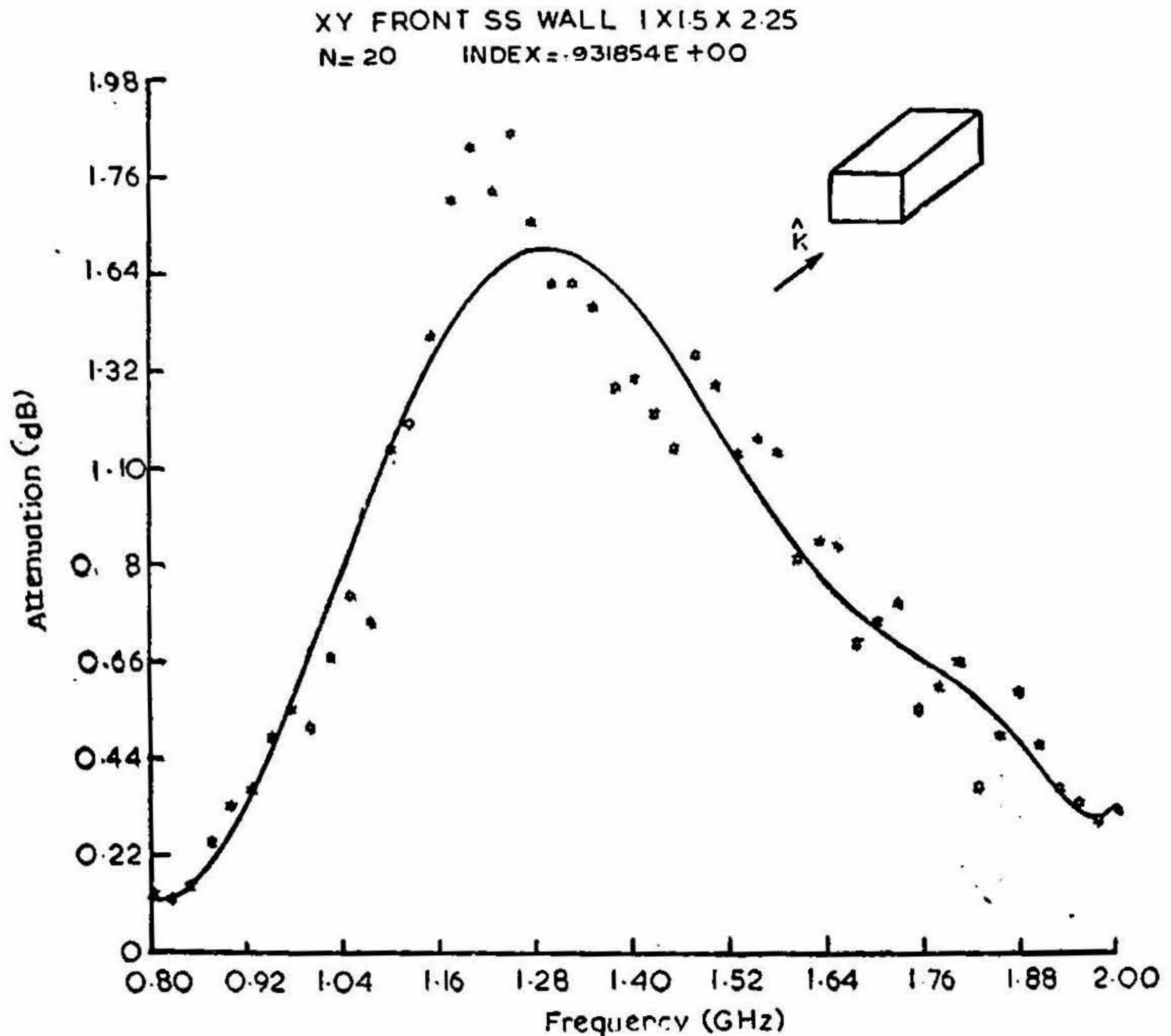

FIG. 18 (d)

In order to see if the enhanced absorption in the vertical orientation translates to a lower exposure time for lethality, 25 gm mice were exposed to plane wave radiation of 150 mW/cm² at 1700 MHz in the $\hat{H} \| \hat{a}$ and $\hat{E} \| \hat{a}$ orientations by rotating the 15·5 dB nominal gain horn antenna through 90°. On the basis of some preliminary results, the average times to lethality* were found to be 500 and 335 seconds, respectively. Noting that the differential

* J. Sharp and J. Schrot, personal communication.

absorption at 1700 MHz is not as large as in the 800–900 MHz region because of the $\hat{E} \parallel \hat{a}$ resonance, experiments in that region should demonstrate a much greater difference in the lethality time, as previously borne out in the heating experiments with the prolate spheroids (*see* Fig. 15).
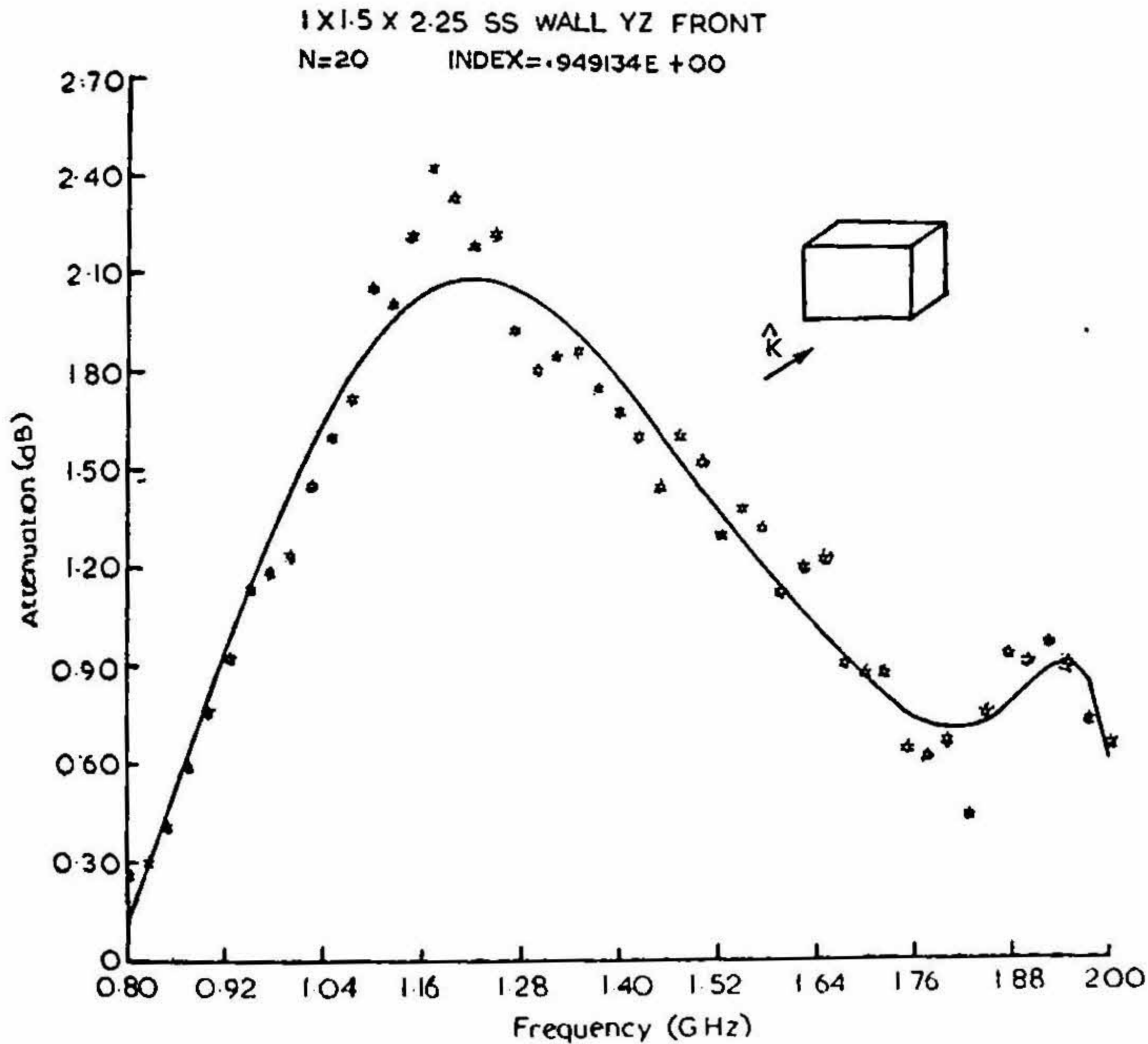

FIG. 18 (*e*)

Differential orientation-dependent RF absorption effects have also been reported in a previous paper by Addington *et al.* [13] In their experiments dogs exposed to 200 MHz radiation in the $\hat{E} \parallel \hat{a}$ configuration were found to experience rectal temperature increases two to three times larger than those exposed in $\hat{H} \parallel \hat{a}$ orientation. Despite their recommendation at the time that this effect be studied further, it seems to have been ignored to our knowledge to this date.

O. P. GANDHI

TABLE V

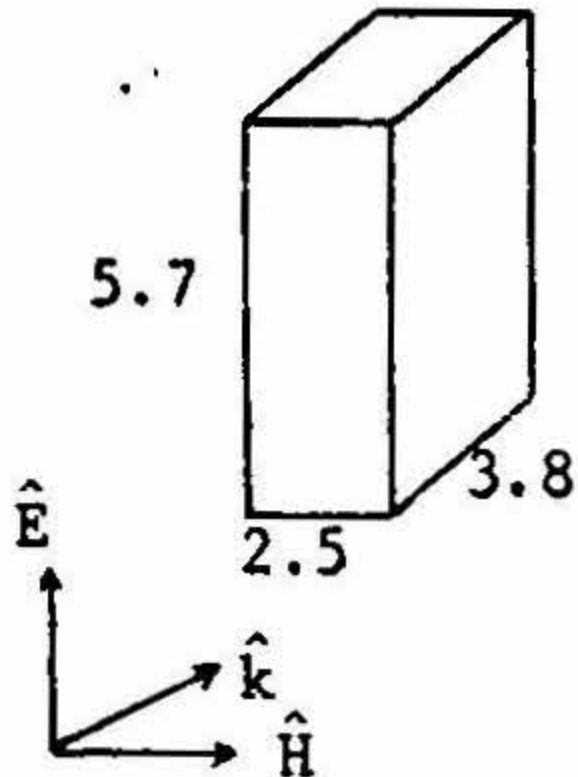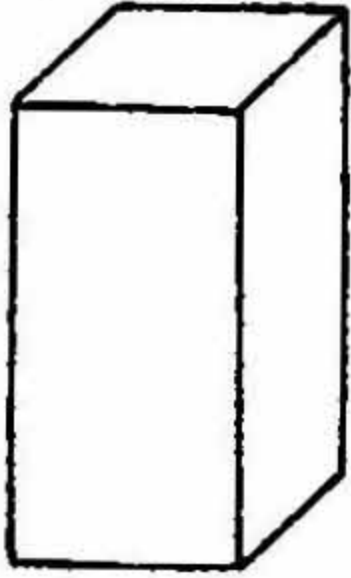*RF absorption characteristics for different orientations of a rectangular parallelepiped*
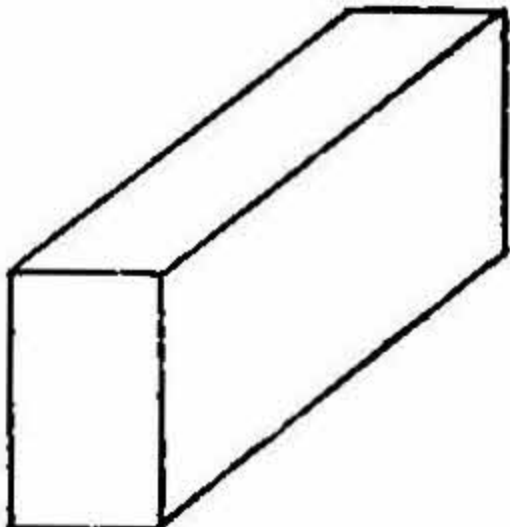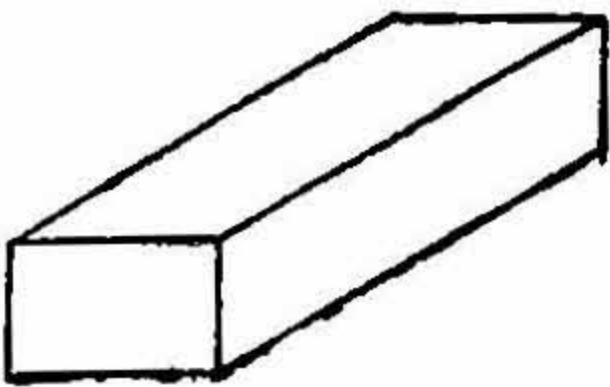
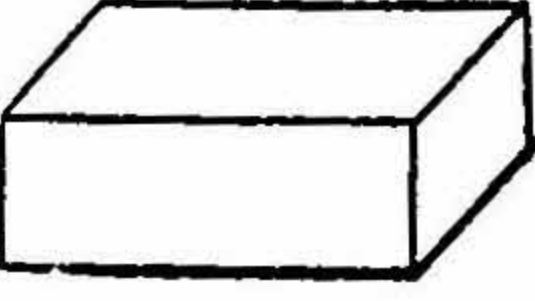| Orientation of the Body	Frequency of Maximum Absorption MHz	Maximum Power Absorption Per cent	$ka \equiv k \times$ (Shadow area)$^{1/2}$	Relative Absorption Coefficient S
1. $\hat{E} \parallel \hat{a}$	960	72·2	0·77	4·98
2.	950	67·4	0·93	3·10
3. $\hat{k} \parallel \hat{a}$	1210	45·0	0·79	4·65

TABLE V—*Contd.*

Orientation of the body	Frequency of Maximum Absorption MHz	Maximum Power Absorption Per cent	$ka \equiv k \times$ (Shadow area)$^{1/2}$	Relative Absorption Coefficient S
4.	1292	30·8	0·84	3·18
5. $\hat{H} \| \hat{a}$	1220	38·0	1·19	1·75
6.	1330	29·5	1·06	2·04

8. SUMMARY AND DISCUSSION OF THE RESULTS

A simple method of measuring wideband RF absorption characteristics of biological systems is described. This takes the shape of a parallel plate waveguide (WG) of cross-sectional dimensions such as to accommodate the animal to fill no more than 10 to 30 per cent of the cross-sectional area at any axial location. This results in an insertion loss larger than about

1dB which helps to reduce by comparison the measurement errors of the network analyzer. The validity of this measuring system has been checked by comparing its results with those of free space irradiation and also from the correlation with Mie theory [1] of the absorption characteristics of different size biological phantom spheres.
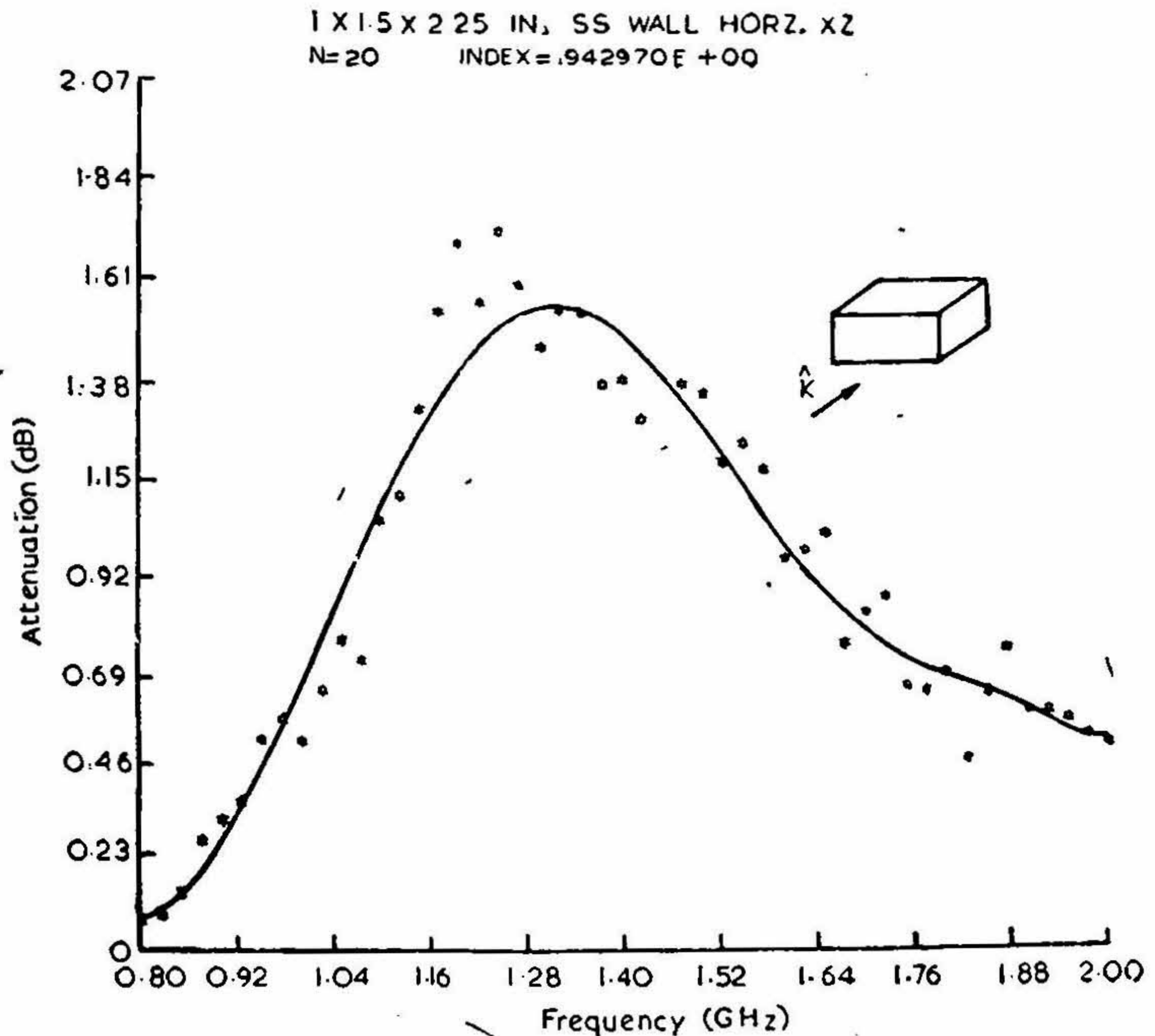

FIG. 18 (f)

The WG is used to measure absorption characteristics in the 285 to 4000 MHz region of 96, 158, 261, and 390 gm Wistar rats placed in the $\hat{k} \parallel \hat{a}$ orientation. Maximum absorption is observed at frequencies of 1217, 1020, 900, and 760 MHz, respectively, with absorption diminishing monotonically (with minor peaks) thereafter to frequencies as high as 4000 MHz. The frequencies of peak absorption and the values thereat demonstrate $W^{1/3}$ and $W^{2/3}$ dependencies upon the weight W of the animal, implying that
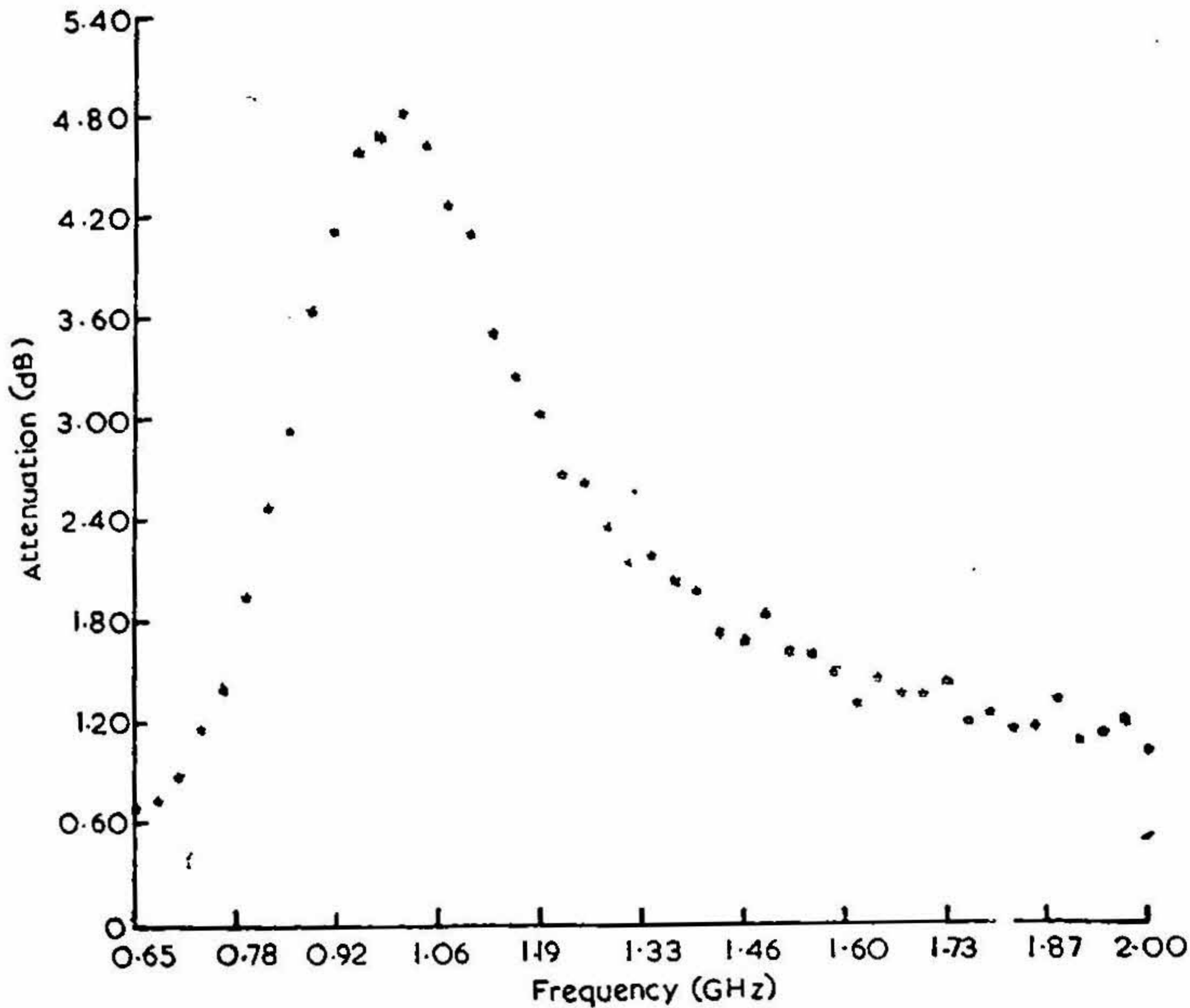
165 GRAM SS MODEL RAT

FIG. 19 (*a*). RF absorption characteristics of full scale models of brain-phantom material for 165 gm and 390 gm rats.

whole animal absorption is a size and shape dependent phenomenon. In subsequent experiments with 25 mg mouse and prolate spheroids, it is shown that such bodies absorb considerably more in the $\hat{E} \parallel \hat{a}$ orientation than in the $\hat{H} \parallel \hat{a}$ configuration with $\hat{k} \parallel \hat{a}$ orientation giving a value only slightly larger than that for $\hat{H} \parallel \hat{a}$ configuration. It is also shown that prolate spheroids and animals* have the lowest resonance frequency for $\hat{E} \parallel \hat{a}$ than for $\hat{k} \parallel \hat{a}$ and $\hat{H} \parallel \hat{a}$ configurations, in that order.

* Experiments to date have been performed only with 25 gm mouse because the dimensions of the present are RG too small to allow $H^+ a$ and $k^+ a$ configurations of the rats.

RF absorption at resonance, larger by an order of magnitude or more, may therefore occur for $\hat{E} \parallel \hat{a}$ orientation than for other configurations of the body. There is a definite frequency region at which this would occur for each of the animals, and this region can be identified using the approach outlined in this paper. Appropriately larger or smaller parallel plate wave-guides would need to be fabricated so that the animal/s to be measured can be placed therein in the three orientations or any other intermediate configuration. Important features of the parallel plate waveguide results are borne out by alternative experiments with free space irradiation.
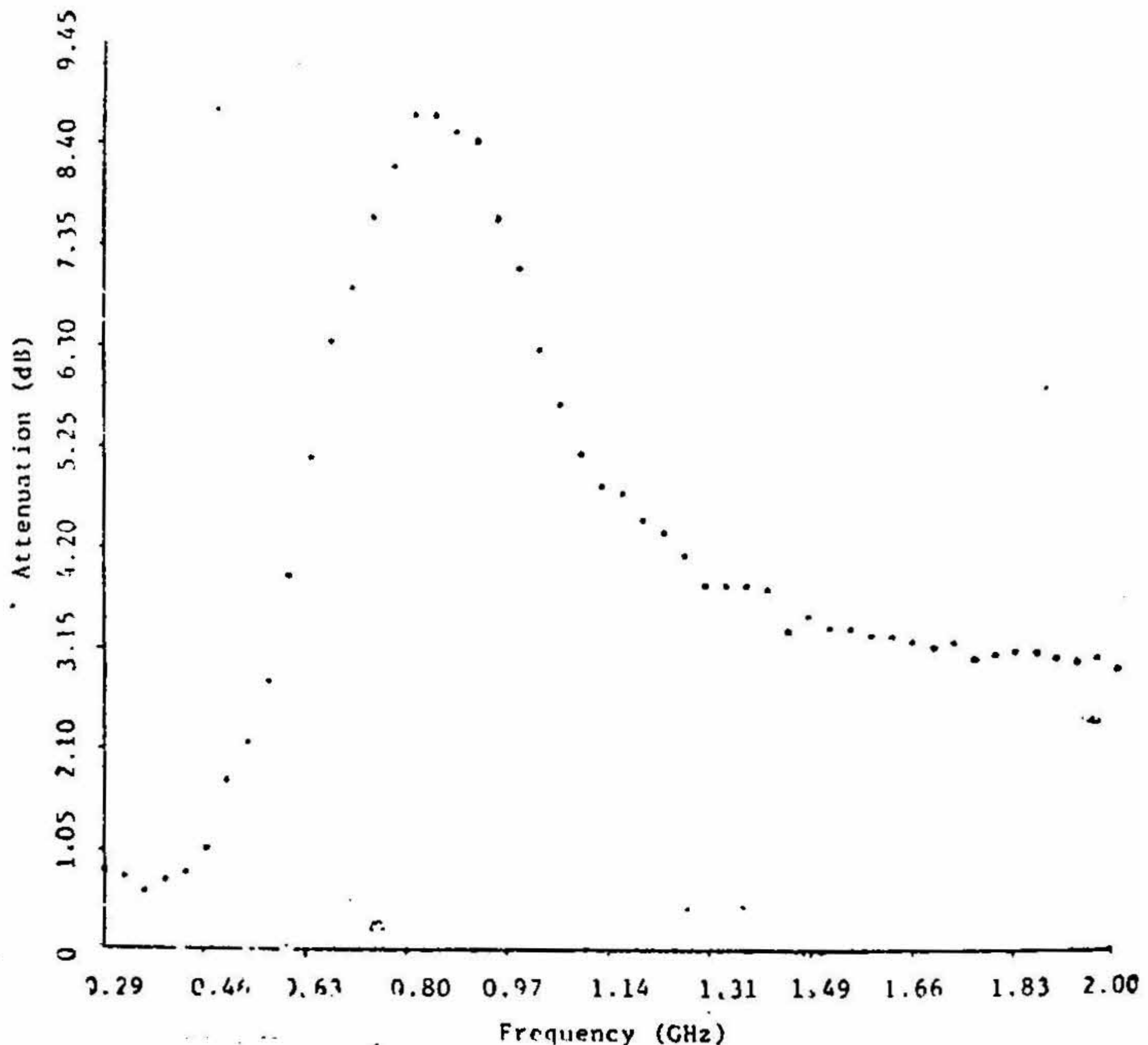
390 GRAM SS MODEL RAT

FIG. 19 (b)

For rats the measured data are in quantitative agreement with results of the behavioral experiments [6]. The absorption at 1700 MHz is more than that at 2450 MHz, which in turn is larger than the value at 3000 MHz. In behavioral experiments, the time to work stoppage was found to be in the
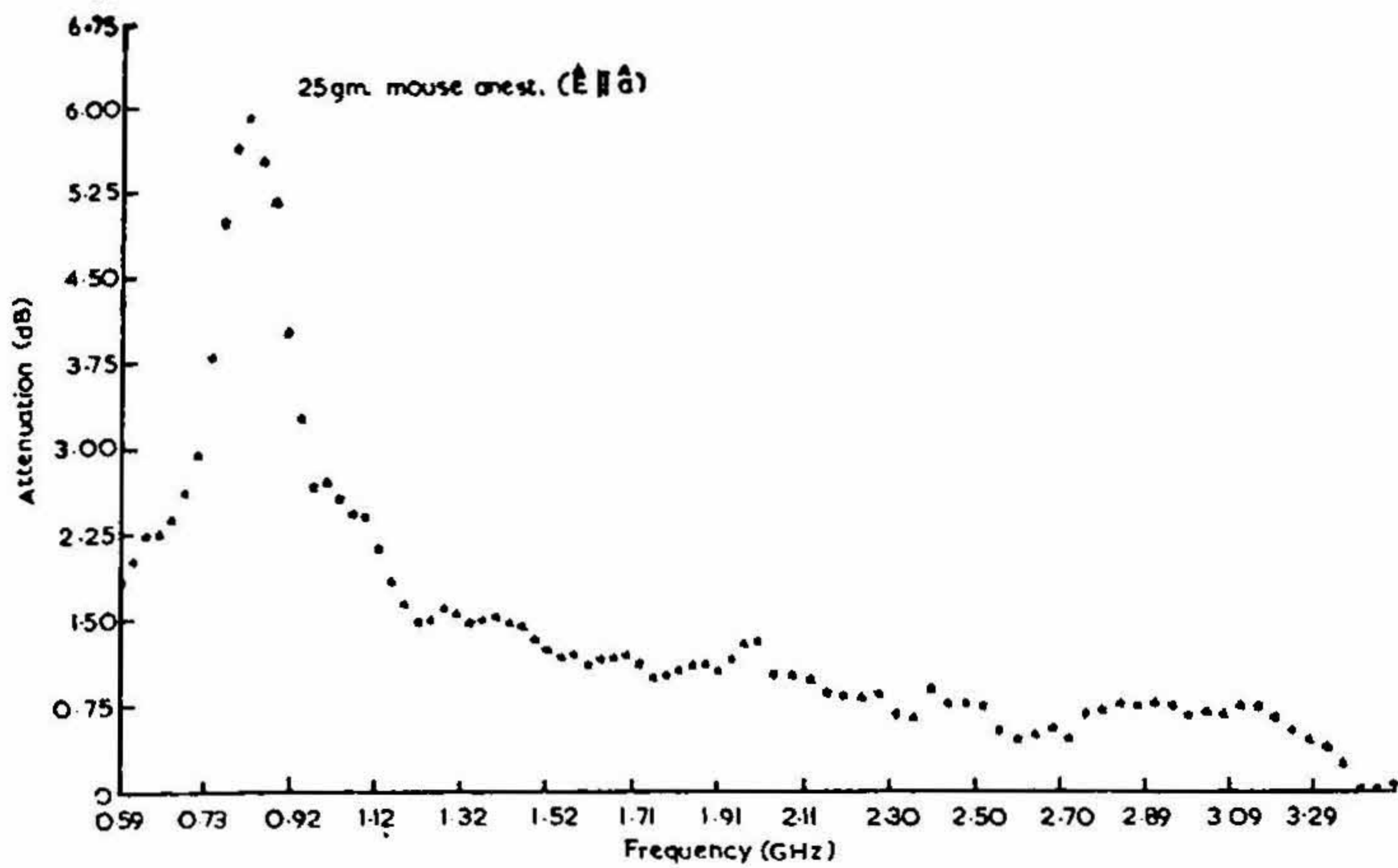
FIG. 20 (a). Absorption characteristics of 25 gm mouse in $\hat{E} \parallel \hat{a}$ orientation.

25 gm MOUSE $(\hat{k} \parallel \hat{a})$
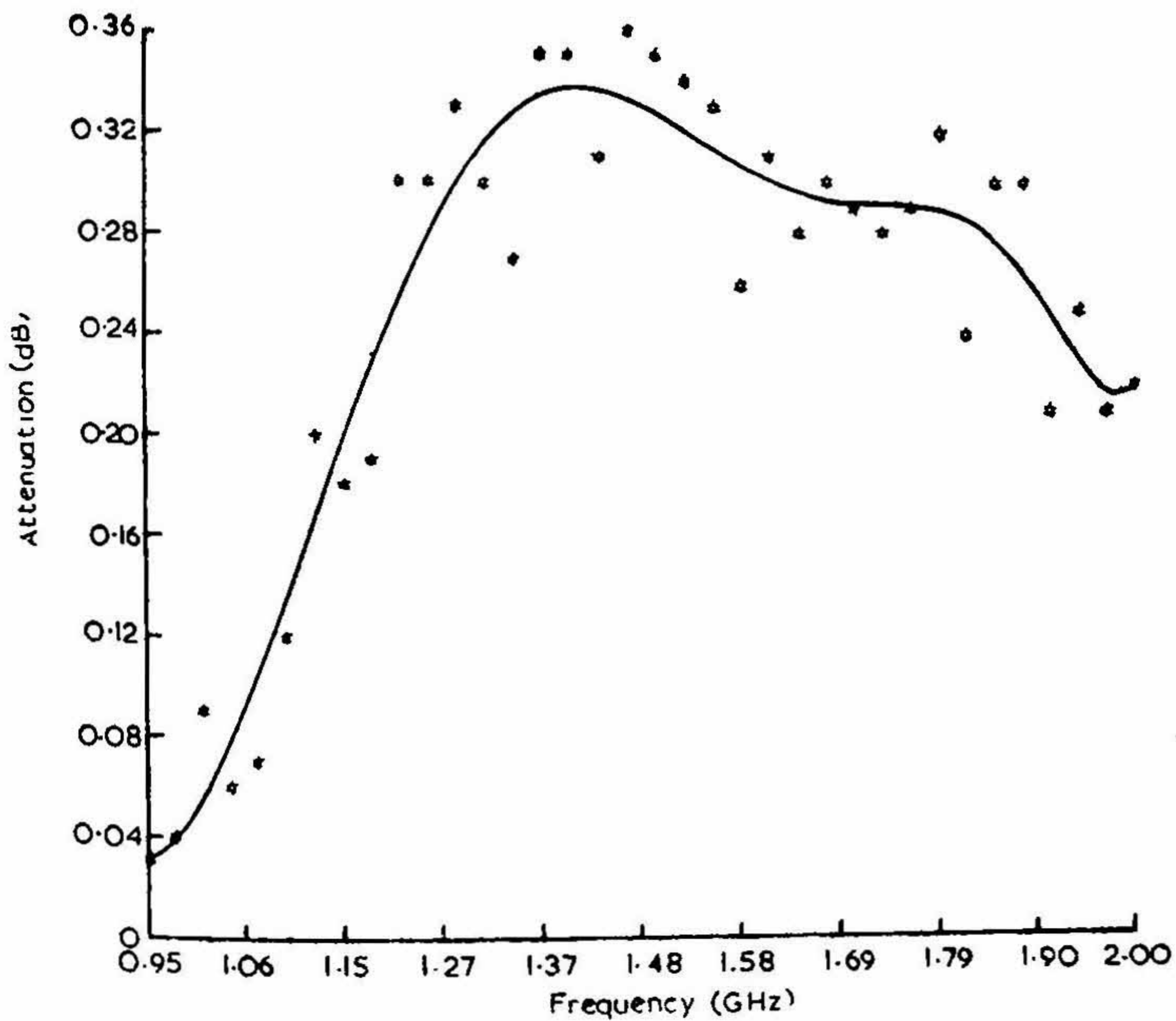N = 14   INDEX = ·920464 E 400

FIG. 20 (b). Absorption characteristics of 25 gm mouse in $\hat{k} \parallel \hat{a}$ orientation.

reverse relationship with that at 1700 MHz being the lowest of the three frequencies. The fact that time to work stoppage was higher, too, at 750 MHz can be explained by noting that the animal orientation was mostly $\hat{H} \parallel \hat{a}$ in the behavioral experiments. This would result in somewhat increased resonance frequencies as compared to the values for the $\hat{k} \parallel \hat{a}$ orientation used in the WG experiments with rats. Since the absorption on the low frequency side of resonance drops off quite rapidly, a lower power absorption at 750 MHz would indeed result for rats compared to the next frequency of 1700 MHz used in the behavioral experiments. From the foregoing it is obvious that the behavioral experiments for rats in the 300–500 MHz band (which should first be identified accurately by the WG method as the band for $\hat{E} \parallel \hat{a}$ resonance) should yield dramatic results for the orientation/
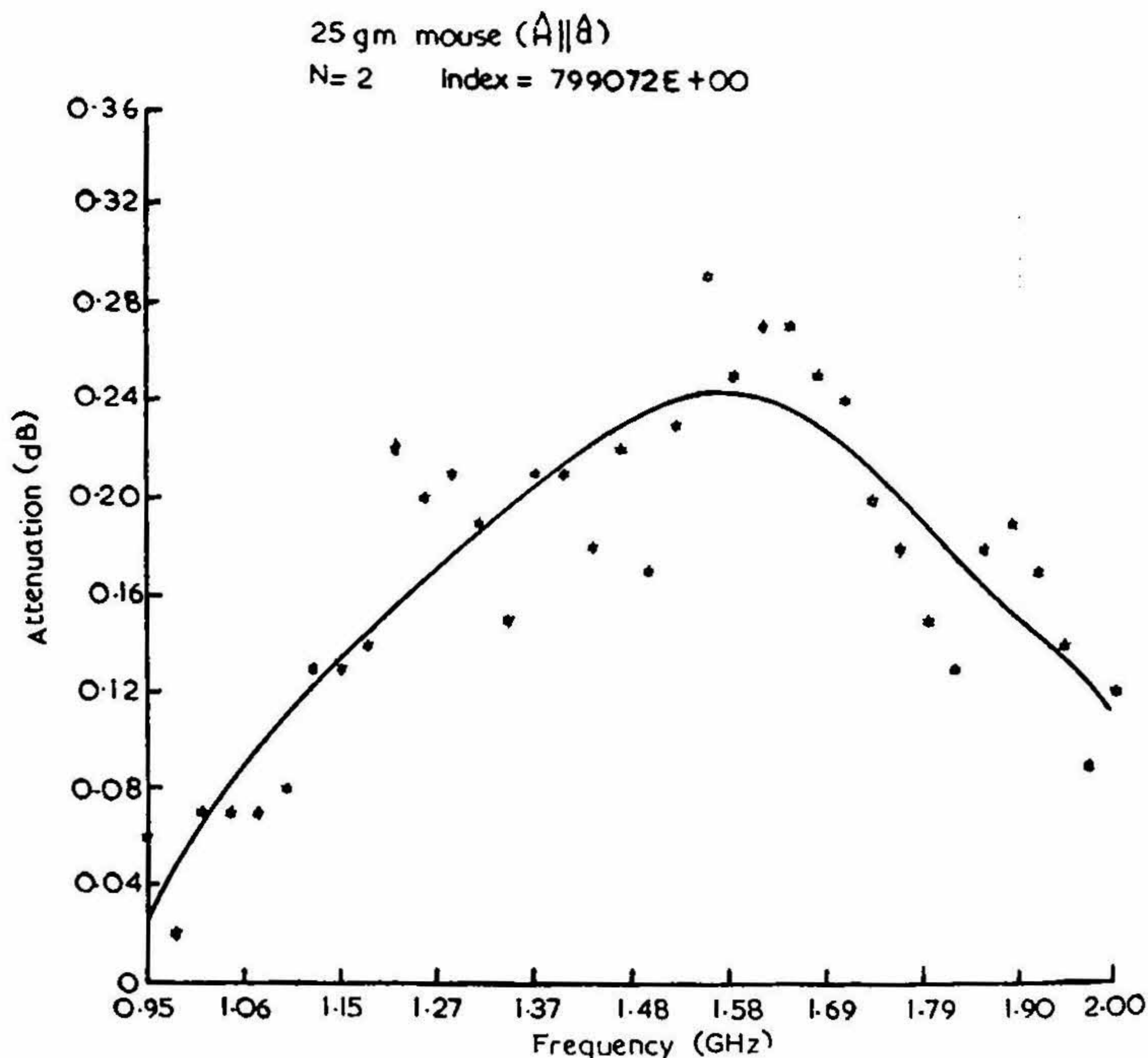
FIG. 20 (c). Absorption characteristics of 25 gm mouse in $\hat{H} \parallel \hat{a}$ orientation.

frequency effects on such animals. For mice the frequency region to study would be the 800–1000 MHz band.

In this paper we have shown that carefully sculptured full scale models of rats of the brain-phantom material gave the RF absorption characteristics fairly similar to those of live animals. The peak absorption frequencies for the 165 and 390 gm models being 1020 and 810 MHz, respectively, correlate exceptionally well with the values 1020 and 760 MHz measured for 158 and 390 gm live rats. On the basis of experiments performed with bodies of prolate spheroidal shapes, the $\hat{E} \parallel \hat{a}$ resonance is found for $ka = 0 \cdot 75$ to 1, while the peaks of absorption for the $\hat{k} \parallel \hat{a}$ and $\hat{H} \parallel \hat{a}$ configurations occur for $ka \simeq a/2b = 2 \cdot 5$ to $3 \cdot 0$ for bodies with aspect ratios between 5 and 6, corresponding to humans. For man with a nominal height $2a$ of 175 cm, the frequency regions corresponding to the above ka values would be 40 to 55 MHz for $\hat{E} \parallel \hat{a}$ resonance and 135 to 165 MHz for peak absorption in the other two configurations. These frequency regions ought to be carefully studied in the context of maximum RF absorption by humans. Since experiments with full size models of man may be difficult because of the correspondingly large WG dimensions that would then be required, reduced scale sculptured models of man may therefore be measured in the first instance with the arrangement described in this paper. From electromagnetic field theory, a body reduced by a factor α in all dimensions would result in the RF characteristic identical to those of the full scale body but at frequencie-scaled up by the factor α. It is necessary, however, that the complex permittis vity presented by the scaled down model correspond to the value at the lower frequencies characteristic of the full body. Since the 40 to 55 MHz band appears appropriate in connection with the $\hat{E} \parallel \hat{a}$ resonance for humans, the reduced scale models should be made of material that closely simulates the permittivity (at least the loss tangent) characteristics of man in this frequency band. It should be recalled that prolate spheroidal bodies in the $\hat{E} \parallel \hat{a}$ orientation, for the frequency region corresponding to the peak for this configuration, have been shown (by several alternative experiments in this paper) to be capable of RF absorption an order of magnitude or more larger than for other orientations. The region of 40 to 55 MHz may therefore be particularly important in the context of humans and deserves careful evaluation.

364 O. P. GANDHI

ACKNOWLEDGEMENT

The author is indebted to Joseph Sharp and H. Mark Grove for their support during his stay at Walter Reed. The assistance of Thomas Andrews and Peter Brown in several facets of this work is greatly appreciated.

REFERENCES

[1] Johnson, C. C and Guy, A. W. — Nonionizing electromagnetic wave effects in biological materials and systems, *Proceedings of the IEEE*, 1972, 60, 692–718.

[2] Kritikos, H. N. and Schwan, H. P. — Hot spots generated in conducting spheres by electromagnetic waves and biological implications, *IEEE Transactions on Biomedical Engineering*, Vol. BME-1972, pp. 53–58.

[3] Anne, A., Satio, M. Salati, O. M. and Schwan, H. P. — Relative microwave absorption cross sections of biological significance, pp 153–177 in Vol. 1 of *Biological Effects of Microwave Radiation*, Plenum Press, 1960.

[4] Stratton, J. A. — *Electromagnetic Theory*, McGraw-Hill Book Company, New York, 1941, 563–567.

[5] Durney, C. H. and Johnson, C. C. — To be published.

[6] Hawkins, T. D., Grove, H. M., Heiple, T. W. and Schrot, J. — Some biological effects of microwave irradiation in the Rat, to be published.

[7] Wheeler, H. A. — Transmission-line properties of parallel strips separated by a dielectric sheet, *IEEE Transactions on Microwave Theory and Techniques*, Vol. MTT-13, 1965, pp. 172–185.

[8] Caulton, M., Hughes, J. J. and Sobol, H. — Measurements on the properties of microstrip transmission lines for microwave integrated circuits, *RCA Review*, 1966, 377–391.

[9] VanKoughnett, A. L. and Wyslouzil, W. — A waveguide TEM mode exposure chamber, *Journal of Microwave Power*, 1972, 7, 381–383.

[10] Frazer, J. W., Mitchell, J. C., Gass, A. E. and Hurt, W. D. — Ghosts and witchcraft in RF measurements or power absorption measurements in RF fields, *Digest of Papers, Joint U.S. Army/Georgia Institute of Technology Microwave Dosimetry Workshop*, Walter Reed Army Institute of Research, Washington D.C., June 1972, 56–73.

[11] Selby, S. M. and Girling, B. — *Standard Mathematical Tables*, Fourteenth Edition. The Chemical Rubber Company, 1965, 469.

[12] Senior, T. B. A. and Goodrich, R. F. — Scattering by a sphere, *Proceedings of the IEE*, 1964, 111, 907–916.

[13] Addington, C. H., Osborn, C., Swartz, G., Fischer, F. P., Newbauer, R. A. and Sarkees, Y. T. — Biological effects of microwave energy at 200 MHz, pp. 177–186 in Vol. 1 of *Biological Effects of Microwave Radiation* Plenum Press, 1960.